

F
N
P

JOURNAL
OF
FOOD
PROCESS
ENGINEERING

D.R. HELDMAN
and
R.P. SINGH
COEDITORS

FOOD & NUTRITION
PRESS, INC.

VOLUME 10, NUMBER 2

QUARTERLY

JOURNAL OF FOOD PROCESS ENGINEERING

- Coeditors:** **D.R. HELDMAN**, National Food Processors Association, 1401 New York Ave., N.W., Washington, D.C.
R.P. SINGH, Agricultural Engineering Department, University of California, Davis, California.
- Editorial Board:** **A.L. BRODY**, Princeton, New Jersey
SOLKE, BRUIN, Vlaardingen, 1 Nederland
A. CALVELO, La Plata, Argentina
M. CHERYAN, Urbana, Illinois
J.P. CLARK, Chicago, Illinois
R.L. EARLE, Palmerston, North New Zealand
B. HALLSTROM, Lund, Sweden
J.M. HARPER, Fort Collins, Colorado
H. HAYASHI, Tokyo, Japan
M. KAREL, Cambridge, Massachusetts
H.G. KESSLER, Freising-Weihenstephan F.R. Germany
C.J. KING, Berkeley, California
J.L. KOKINI, New Brunswick, New Jersey
M. LEMAGUER, Edmonton, Alberta, Canada
R.G. MORGAN, E. Lansing, Michigan
M. PELEG, Amherst, Massachusetts
M.A. RAO, Geneva, New York
I. SAGUY, Minneapolis, Minnesota
S.K. SASTRY, Columbus, Ohio
W.E.L. SPIESS, Karlsruhe, Germany
J.F. STEFFE, East Lansing, Michigan

All articles for publication and inquiries regarding publications should be sent to either DR. D.R. HELDMAN, COEDITOR, *Journal of Food Process Engineering*, National Food Processors Association, 1401 New York Ave., N.W., Washington, D.C. 20005 USA; or DR. R.P. SINGH, COEDITOR, *Journal of Food Process Engineering*, University of California, Davis, Department of Agricultural Engineering, Davis, CA 95616 USA.

All subscriptions and inquiries regarding subscription should be sent to Food & Nutrition Press, Inc., 6527 Main Street, P.O. Box 583, Trumbull, Connecticut 06611 USA.

One volume of four issues will be published annually. The price for Volume 10 is \$80.00 which includes postage to U.S., Canada, and Mexico. Subscriptions to other countries are \$94.00 per year via surface mail, and \$102.00 per year via airmail.

Subscriptions for individuals for their own personal use are \$60.00 for Volume 10 which includes postage to U.S., Canada, and Mexico. Personal subscriptions to other countries are \$74.00 per year via surface mail, and \$82.00 per year via airmail. Subscriptions for individuals should be sent to the publisher and marked for personal use.

The *Journal of Food Process Engineering* (ISSN 0145-8375) is published quarterly (March, June, September and December) by Food & Nutrition Press, Inc.—Office of Publication is 6527 Main Street, P.O. Box 583, Trumbull, Connecticut 06611 USA. (Current issue is August 1988.)

Second class postage paid at Bridgeport, CT 06604.

POSTMASTER: Send address changes to Food & Nutrition Press, Inc., 6527 Main Street, P.O. Box 583, Trumbull, CT 06611.

JOURNAL OF FOOD PROCESS ENGINEERING

JOURNAL OF FOOD PROCESS ENGINEERING

Coeditors:

D.R. HELDMAN, National Food Processors Association, 1401 New York Ave., N.W., Washington, D.C.

R.P. SINGH, Agricultural Engineering Department, University of California, Davis, California.

Editorial Board:

A.L. BRODY, Schotland Business Research, Inc., Princeton Corporate Center, 3 Independence Way, Princeton, New Jersey

SOLKE, BRUIN, Unilever Research Laboratorium, Vlaardingen, Oliver van Noortland 120 postbus 114, 3130 AC Vlaardingen 3133 AT Vlaardingen, 1 Nederland

A. CALVELO, Centro de Investigacion y Desarrollo en Criotechnologia de Alimentos, Universidad Nacional de la Plata, Argentina

M. CHERYAN, Department of Food Science, University of Illinois, Urbana, Illinois.

J.P. CLARK, Epstein Process Engineering, Inc., Chicago, Illinois

R.L. EARLE, Department of Biotechnology, Massey University, Palmerston North, New Zealand

B. HALLSTROM, Food Engineering Chemical Center, S-221 Lund, Sweden

J.M. HARPER, Agricultural and Chemical Engineering Department, Colorado State University, Fort Collins, Colorado

H. HAYASHI, Snow Brand Milk Products Co., Ltd., Shinjuku, Tokyo, Japan

M. KAREL, Department of Applied Biological Sciences, Massachusetts Institute of Technology, Cambridge, Massachusetts

H.G. KESSLER, Institute for Dairy Science and Food Process Engineering, Technical University Munich, Freising-Weihestephan, F.R. Germany

C.J. KING, Department of Chemical Engineering, University of California, Berkeley, California

J.L. KOKINI, Department of Food Science, Rutgers University, New Brunswick, New Jersey

M. LEMAGUER, Department of Food Science, University of Alberta, Edmonton, Canada

R.G. MORGAN, Department of Food Science and Human Nutrition, Michigan State University, E. Lansing, Michigan

M. PELEG, Department of Food Engineering, University of Massachusetts, Amherst, Massachusetts

M.A. RAO, Department of Food Science and Technology, Institute for Food Science, New York State Agricultural Experiment Station, Geneva, New York

I. SAGUY, The Pillsbury Co., Minneapolis, Minnesota

S.K. SASTRY, Department of Agricultural Engineering, Ohio State University, Columbus, Ohio

W.E.L. SPIESS, Bundesforschungsanstalt fuer Ernaehrung, Karlsruhe, Germany

J.F. STEFFE, Department of Agricultural Engineering, Michigan State University, East Lansing, Michigan

**Journal of
FOOD PROCESS ENGINEERING**

**VOLUME 10
NUMBER 2**

**Coeditors: D. R. HELDMAN
R.P. SINGH**

**FOOD & NUTRITION PRESS, INC.
TRUMBULL, CONNECTICUT 06611 USA**

© Copyright 1988 by
Food & Nutrition Press, Inc.
Trumbull, Connecticut USA

All rights reserved. No part of this publication may be reproduced, stored in a retrieval system or transmitted in any form or by any means: electronic, electrostatic, magnetic tape, mechanical, photocopying, recording or otherwise, without permission in writing from the publisher.

ISSN 0145-8876

Printed in the United States of America

RESIDENCE TIME DISTRIBUTION IN HORIZONTAL THIN FILM SCRAPED SURFACE HEAT EXCHANGER (SSHE)

H. ABICHANDANI and S. C. SARMA

*Dairy Engineering Division
National Dairy Research Institute
Karnal 132 001 (India)*

Accepted for Publication October 3, 1987

ABSTRACT

The residence time distribution (RTD) studies were conducted to predict the flow characteristics in thin film SSHE. The experiments were conducted at zero heat flux using water as working fluid. A pulse input in form of saturated sodium chloride solution was used as the disturbance at inlet and the response in form of electrical conductivity was measured at outlet. Thirty-two trials were conducted at different flow rates, number of blades and rotor speeds. The E-curves were plotted. It was inferred that the flow in thin film SSHE approximates to plug flow. Also, as the mass flow rate increased, RTD improved. The increasing number of blades resulted in appreciable improvement in RTD. The rotor speed had similar effect as that of number of blades on RTD. However, the number of blades had more profound effect as compared to rotor speed. If the rotor design is modified then RTD can be improved and simultaneously the power consumption can be kept at minimum.

INTRODUCTION

When a process fluid is heated continuously by directing it through a heat exchanger, not all liquid particles are heated for same length of time. This is because of what is called residence time distribution (RTD). In order to facilitate the design of process equipment, understanding flow characteristics is of paramount importance. Among the approaches to this end, study of residence time distribution seems to be most useful.

Generally, flow pattern is examined in the perspective of two ideal situations which are opposite to each other. If the flow in the heat exchanger is such that velocity

distribution is flat across the flow passage, the system is said to be under plug flow condition. In this case, there is no spread of residence time. On the other hand, the complete mixing implies that the properties of medium are uniform inside the heat exchanger including those at the outlet. It is obvious that a real system will not behave exactly as a plug flow or completely mixed one and very often deviates quite significantly from both. However, theoretically, as the number of completely mixed vessels connected in series increases to infinity, the system approaches a plug flow.

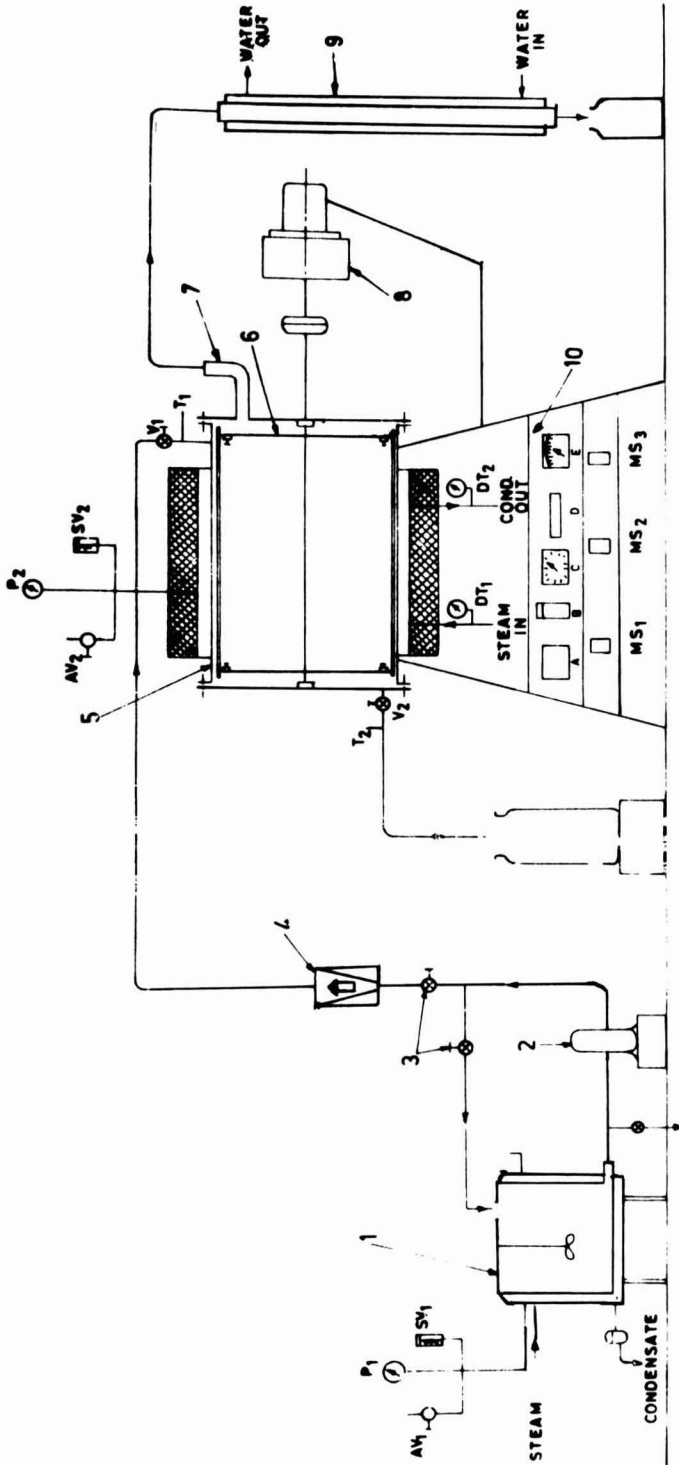
Lin (1979) has discussed theory of residence time distribution of flow and its application in estimation of the sterilization efficiency of process equipment. It was concluded that for flows in equipments such as plate heat exchangers and scraped surface heat exchangers which have either complex channel geometries or moving accessory along the flow passage, experimental determination of the residence time distribution is necessary because the flow patterns in them become too complicated to be adequately described by a mathematical model. Danckwerts (1953), Levenspiel (1962), Freeze and Glover (1979) studied the RTD in vertical thin film scraped surface heat exchangers (0.025 m to 0.1 m diameter and 0.5 to 0.8 m length). However, no adequate information is available on RTD in horizontal thin film SSHEs.

The purpose of present study is to discuss the RTD in straight-sided horizontal thin film SSHE and also to examine the effect of various variables viz. mass flow rate, number of blades and rotor speed on the RTD.

MATERIALS AND METHODS

The schematic hook-up of experimental set up is shown in Fig. 1. The study was carried out under isothermal conditions at zero heat flux. The water was filled in feed tank (1) at room temperature and then pumped through a lob-type positive displacement pump (2) into the heat exchanger (5). The regulating valves (3) were adjusted until the desired flow rate was achieved as shown by rotameter (4). The variable speed drive (7) was energized and the rotor's (6) speed was adjusted by means of manual speed controller. The rotor was provided with swinging type scraper blades. Due to the centrifugal action of blades, the fluid spreads over the heat transfer surface in form of a thin film. Saturated sodium chloride solution (5 mL) as tracer was injected at the inlet in form of a pulse (stimulus). Samples were drawn from the outlet stream at periodic intervals of 5 s. The conductivity of these samples i.e., responses were measured by the conductivity bridge.

The hold-up volume inside the heat exchanger for a particular flow rate, number of blades and rotor speed, was measured by suddenly stopping the pump motor and then immediately collecting the liquid in a measuring container. Sufficient precautions were observed to ensure the volume of liquid collected was exclusive



1. FEED TANK. 2. FEED PUMP. 3. FLOW REGULATION VALVES. 4. ROTAMETER. 5. HEAT EXCHANGER. 6. SCRAPER. 7. VAPOUR OUTLET
 8. VARIABLE SPEED DRIVE. 9. CONDENSER 10. INSTRUMENT PANEL. A - ELECTRONIC REGULATOR. B - MANUAL SPEED CONTROLLER.
 C - SELECTOR SWITCH. D - MILLIVOLT METER. E - WATT METER. V_1 & V_2 - INLET AND OUTLET VALVES. T_1 & T_2 - INLET AND OUTLET
 THERMO-WELLS. MS_1 , MS_2 AND MS_3 - MOTOR STARTERS. AV_1 & AV_2 - AIR VENTS. P_1 & P_2 - PRESSURE GAUGES. DT_1 & DT_2 - DIAL THER-
 MOMETERS. SV_1 & SV_2 - SAFETY VALVES.

FIG. 1. SCHEMATIC DIAGRAM OF EXPERIMENTAL SET-UP

of that flowing in interconnecting pipes. The tracer was then evenly mixed in each hold-up volume and the conductivity was measured. This conductivity is termed as mean conductivity (\bar{C}). The mean residence time (\bar{t}) is the ratio of hold-up volume to the volumetric flow rate of liquid. Thirty two experiments were conducted.

On the basis of diameter of experimental heat exchanger (0.34 m) which was large when compared to those in the literature, the rotor speed was kept in range 1.67 to 5 rps to obtain rotational Reynold's number of 3.8×10^5 to 11.7×10^5 . The length of heat exchanger was 0.76 m. Material of construction was 304-stainless steel.

Flow rate of water was varied from .025 to 0.062 kg/s, thereby film Reynold's number ranged from 170 to 470.

Number of blades (variable clearance type) employed in the study were 2, 4, 6 and 8. Details of blades were as follows:

Mass	—	0.114 kg/blade
Length	—	.069 m
Width	—	0.0135 m
Thickness	—	0.00175 m
Material	—	304-stainless steel

RESULTS AND DISCUSSION

In the pulse form of disturbance, a tracer is injected for a short time at $t = 0$ and change in concentration at the outlet is measured. If the observations are plotted in terms of dimensionless concentration (C/\bar{C}) and time (t/\bar{t}), the resulting graph is called E diagram (Leniger and Beverloo 1975; and Levenspiel 1974).

For an ideal mixer, it can be shown that:

$$E(t) = \bar{t} \frac{d}{dt} \{F(t)\} \quad (1)$$

where, $F(t)$ is the probability of residence time smaller than or equal to t .

For n -ideal mixers:

$$E(t) = \frac{n^n}{(n-1)!} \left[\frac{t}{\bar{t}} \right]^{n-1} \text{Exp} \left[\frac{-nt}{\bar{t}} \right] \quad (2)$$

As can be seen:

$$\frac{d^2 F(t)}{dt} = \frac{1}{\bar{t}} \frac{d E(t)}{dt} \quad (3)$$

and maximum is obtained by equating either of them to zero. This yields:

$$\frac{t}{\bar{t}} = \frac{n - 1}{n} \quad (4)$$

It can be easily seen that as $n \rightarrow \infty$, $t/\bar{t} \rightarrow 1$ which represents ideal plug flow. Thus, closer the value of t/\bar{t} to unity for which C/\bar{C} is maximum in $E(t)$ diagrams, the flow in the processor is near to the plug flow.

The observed E-curve can also give clues to poor contacting and flow in the process equipment. The defects like channeling, presence of stagnant regions in the processor and fluid channeling down two parallel paths, can easily be detected from E-curves.

The data generated during the experiments are illustrated in Fig. 2 to 5. It is noticed that all curves start at a certain value of C/\bar{C} essentially because of initial conductivity of water. Soft water was used in the experiments.

Effect of Various Parameters on RTD

Mass flow rate, M. Figure 2 illustrates the effect of mass flow rate on RTD with number of blades as 2 and rotor speed 2.5 rps. A mechanism governing fluid flow, film formation and action of rotating blades on heat transfer is explained elsewhere (Abichandani and Sarma 1987). As the mass flow rate was increased, the RTD improved. This could be attributed to higher turbulence in the fillet and of fluid film (the fluid distribution in thin film SSHE is assumed to be in form of a triangular fillet in front of the blade and as film past the tip of blade). At low mass flow rate of 0.025 kg/s (film Reynold's number 170), the fluid seemed to be in form of film only which resulted in less turbulence and hence poor RTD. The maximum mass flow rate of 0.062 kg/S approxiated to $n = 8$ ($t/\bar{t} = 0.87$) of ideally stirred reactors. Thus, it is obvious that the mass flow rate for the SSHE should be so maintained that n is maximum. During sensible heat transfer studies, it was observed that increase in mass flow rate resulted in higher values of scraped film heat transfer coefficient.

Number of Blades, B. Figure 3 shows the effect of number of blades on RTD. The number of blades were varied from 2 to 8, keeping the mass flow rate at 0.025 kg/s at 2.5 rps.

It is interesting to observe the effect of the number of blades on RTD. Higher its number, closer the RTD to plug flow. The closest value of t/\bar{t} to unity occurred with 8 number of blades. The increase in number of blades results in greater degree of turbulence and radial mixing which are equally responsible for improved RTD.

However, the rotor power consumption increases with number of blades. It was also seen during heat transfer studies that increasing the number of blades

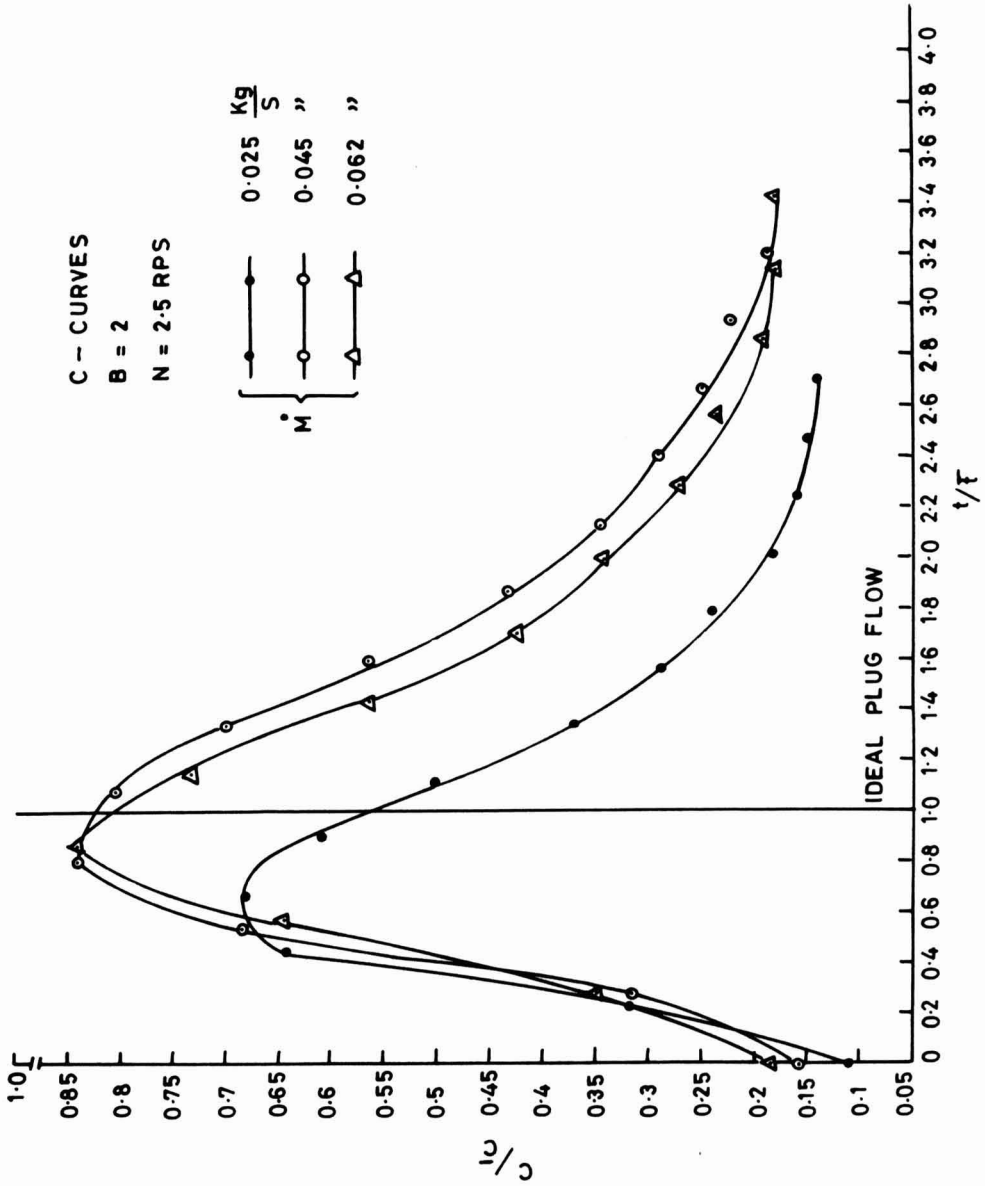


FIG. 2. EFFECT OF M ON R.T.D.

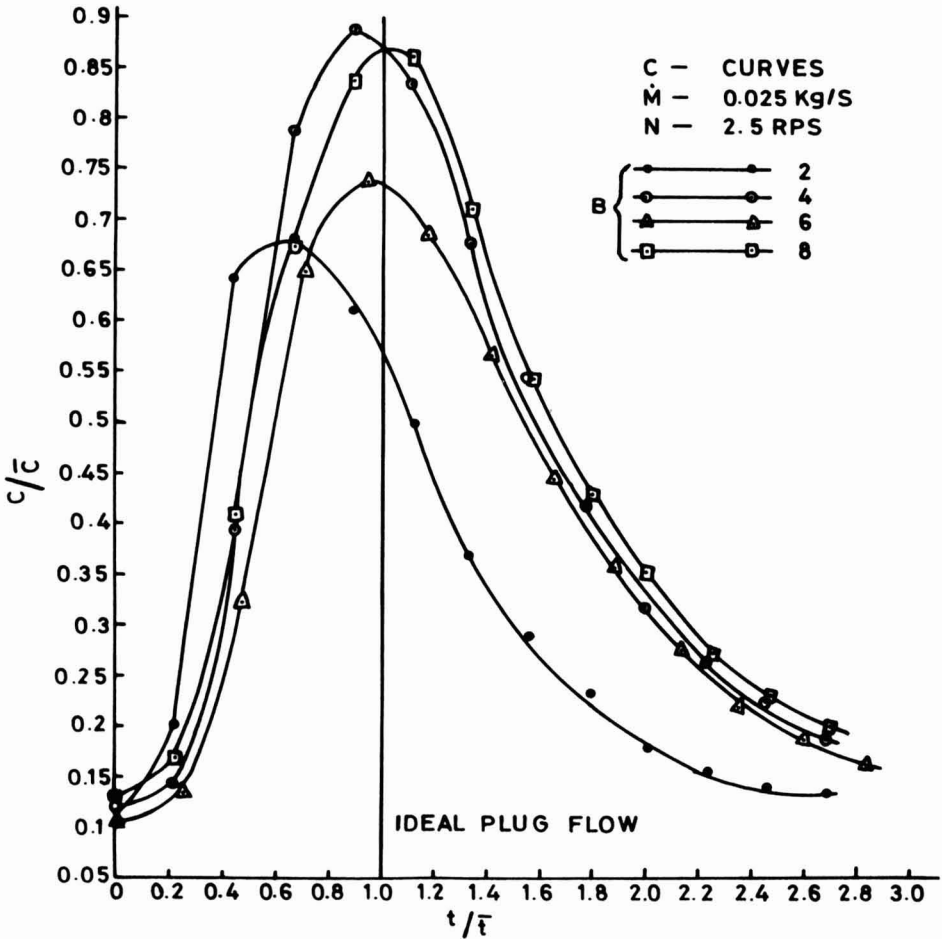


FIG. 3. EFFECT OF B ON R.T.D.

beyond 4 did not appreciably increase film heat transfer coefficient (Abichandani and Sarma 1987). Therefore, it may not be of much advantage to operate the SSHE with blades more than 4 merely to improve the RTD. Thus, there exists a need in redesigning the rotor that gives improved RTD simultaneously keeping power consumption at minimum.

Rotor Speed, N. Figure 4 illustrates the effect of rotor speed on RTD with mass flow rate of 0.025 kg/s and four blades. It was earlier mentioned that increase in rotor speed would cause higher turbulence in fillet and film and its effect is somewhat similar to that obtained from increasing the number of blades. Although the closest values of t/\bar{t} to unity at which C/\bar{C} is maximum, do not vary appreciably; the fact that the peak width of E-curves at higher rotor speeds

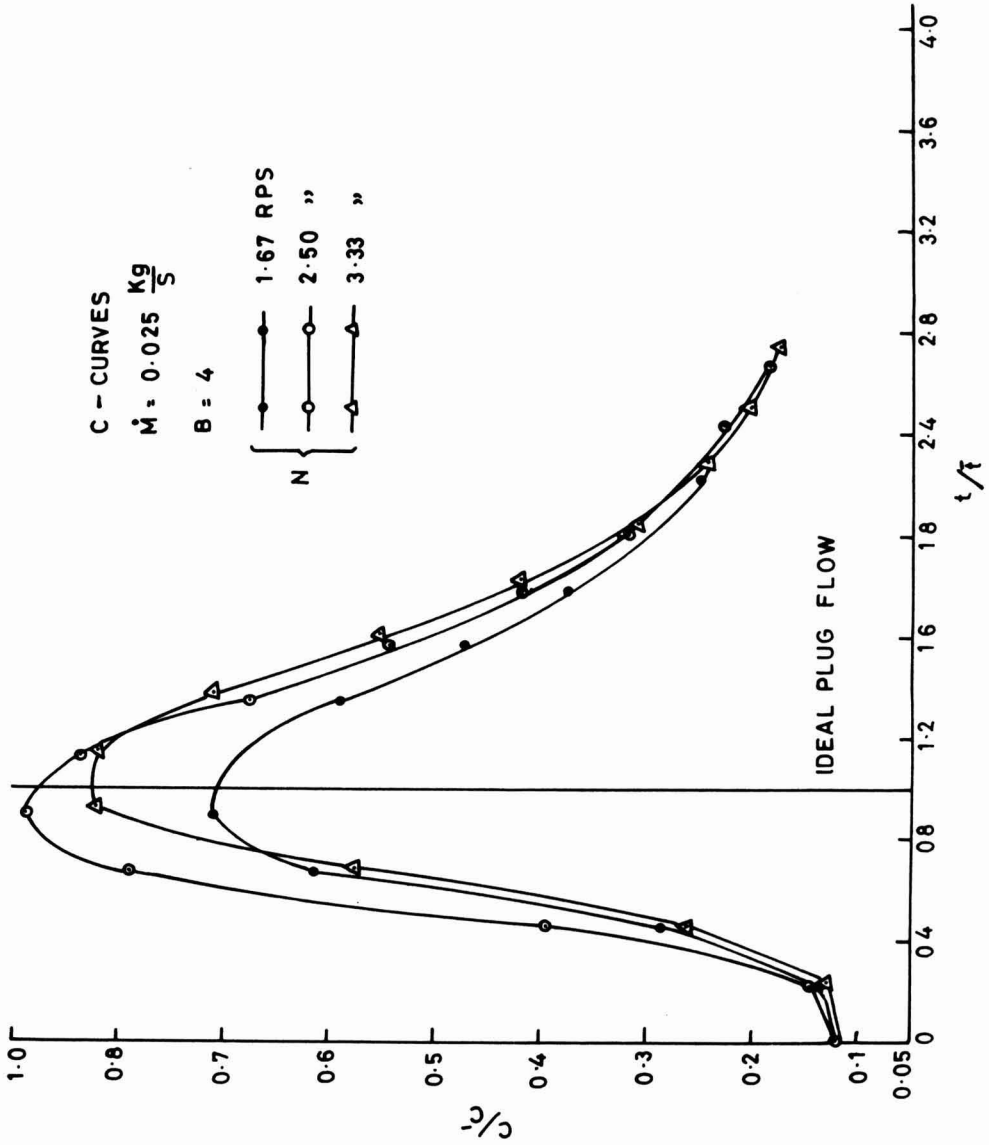


FIG. 4. EFFECT OF N ON R.T.D. (B = 4)

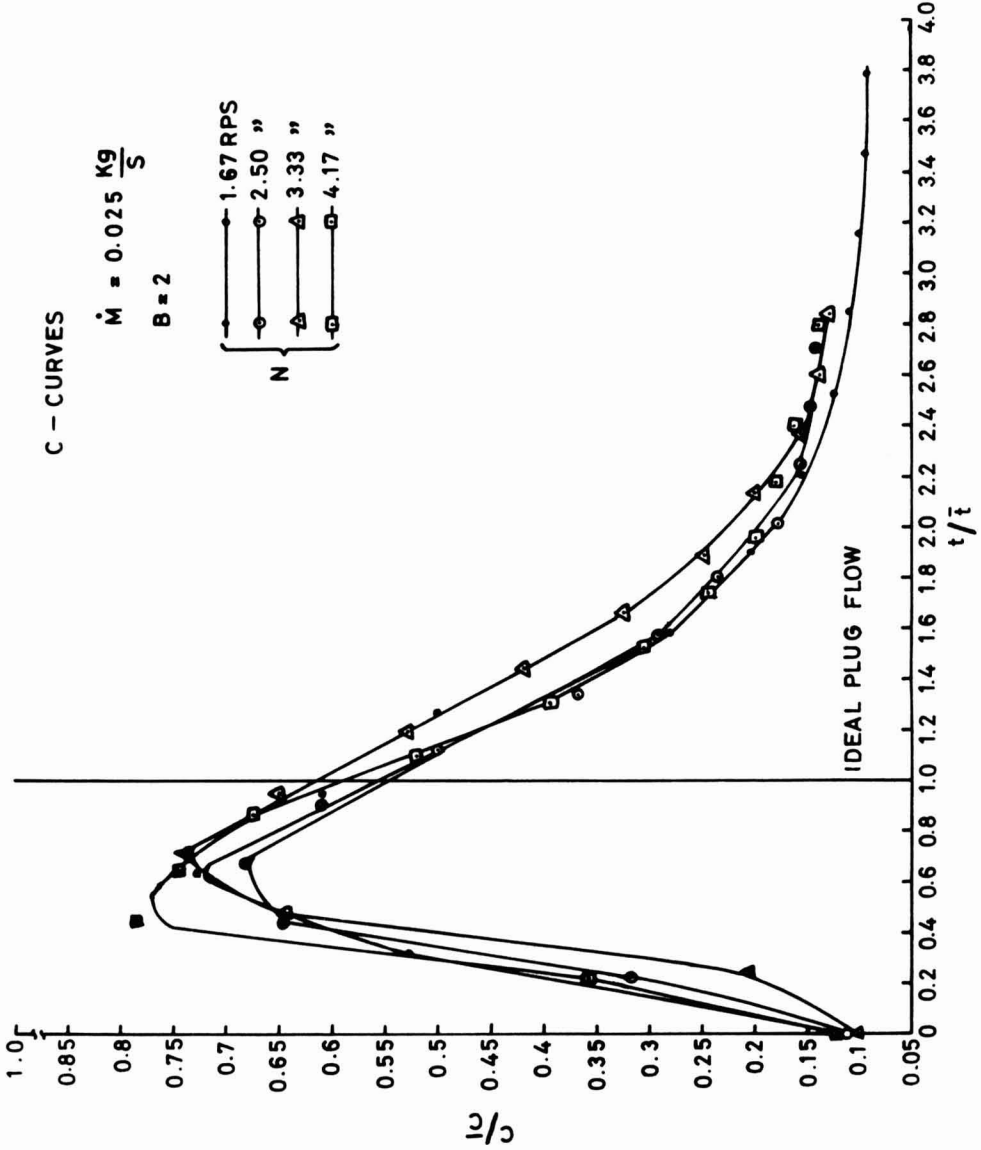


FIG. 5. EFFECT OF N ON R.T.D. (B = 2)

is narrowed, shows improvement in RTD with increased rotor speeds. It is interesting to compare Fig. 3 and 4 and observe that the number of blades have more pronounced effect on RTD as compared to rotor speed as peak widths of curves in former case are relatively narrower. This is obviously due to the increased fillet volume at higher number of blades and more frequent interception of inlet-outlet path which minimizes channeling.

CONCLUSION

The flow pattern in horizontal thin film SSHE is demonstrated. The RTD can be improved by increasing the mass flow rate, number of blades and rotor speed. However, it was found that the number of blades has more profound effect on RTD as compared to the rotor speed. If the rotor design is modified, may be by staggering the blades, then RTD can be improved and simultaneously the power consumption can be kept at minimum.

REFERENCES

- ABICHANDANI, H. and SARMA, S. C. 1987. Heat transfer and power requirements in horizontal thin film scraped surface heat exchangers. *Chem. Eng. Sci.* (In Press).
- DANKWERTS, P. V. 1953. *Chem. Eng. Sci.* 1.
- FREEZE, H. L. and GLOVER, W. B. 1979. Mechanically agitated thin film evaporator. *Chem. Eng. Prog.* (Jan.), 52-58.
- LENIGER, H. A. and BEVERLOO, W. A. 1975. D. Reidel Pub. Co. Boston, MA. *Food Process Engineering*. pp. 44-50.
- LEVENSPIEL, O. 1962 AND 1974. *Chemical Reaction Engineering*. PP. 255-305. Wiley Eastern Pvt. Ltd., New York.
- LIN, S. H. 1979. Residence time distribution of flow in a continuous sterilization process. *Process Biochem.* (July), 23-27.

FREEZING TIME CALCULATION FOR PRODUCTS WITH SIMPLE GEOMETRICAL SHAPES

C. LACROIX and F. CASTAIGNE

*Department de sciences et technologie des aliments
Universite Laval
Ste-Foy, Quebec G1K 7P4*

Accepted for Publication April 5, 1988

ABSTRACT

A simple model is proposed to estimate freezing times of foodstuffs of simple geometrical shapes (infinite flat slabs, infinite cylinders, spheres, rectangular parallelepipeds and finite cylinders). This model combines Plank's equation for change of phase period with the unsteady heat transfer solutions for cooling periods before and after phase change.

The total freezing time is obtained by the determination and the summation of the precooling, phase change and tempering times. The results produced are at least as accurate as or better than any of the previous methods, including regression formula and finite difference computations.

Tables required for fast and accurate predictions of freezing times of foodstuffs with this method are provided.

INTRODUCTION

Freezing is one of the most important methods of food preservation. Many attempts have been made to find a reasonably simple method for predicting freezing times. Freezing of foodstuffs involves unsteady heat transfer with phase change which makes calculation rather complicated. It has been shown that practical freezing problems involve convective cooling at the surface, and initial superheating. Furthermore, during freezing of foods, latent heat, released over a range of temperature and thermal properties in either the frozen or unfrozen phases is not

constant. Because of these problems and the inherent nonlinear boundary conditions, no general analytical solution exists for predicting the freezing times of foodstuffs.

A variety of methods to predict freezing times for foods have been suggested and very good reviews and assessments have recently been published (Ramaswamy and Tung 1984; Cleland and Earle 1984). These can be classified into two groups. The first group are the numerical finite difference and finite element solutions. This approach can handle all types of boundary conditions, shapes and variations in the thermal properties of the freezing material. Although numerical models are more exact, they are difficult to use in practice. They require possession of the appropriate numerical programs and computers, something rarely feasible for the user of these types of calculation. The second group comprises those methods where simplifying assumptions are made. They lead to the solution of partial differential equations to yield completely analytical and explicit formula. Most of these simplified analytical models are based on modifications of Plank's equation (1941), restricted to systems with an initial temperature equal to that of equilibrium, constant properties, pseudo-steady state conduction in the frozen layer and final temperature at the center equal to the initial one.

Numerical corrections have been proposed for Plank's equation, without taking into account sensible heat above freezing (Nagaoka *et al.* 1955; Plank 1963; Cleland and Earle 1977 and 1982; Hung and Thompson 1983), as well as combinations of equations without change of phase (Mascheroni and Calvelo 1982; De Michelis and Calvelo 1982 and 1983). Most of these methods are of limited use or are not sufficiently accurate for design purposes.

In the present report, models are developed for fast and accurate predictions of freezing time for various geometrical shaped products (infinite flat slabs, infinite cylinders, spheres, rectangular parallelepipeds and finite cylinders). Tables required for calculations are provided.

THEORY

The experimental food freezing curve as presented in Fig. 1 can be divided into three different areas:

- (1) a cooling period with unsteady state heat transfer, where the product is cooled from the initial temperature to the beginning of freezing temperature.
- (2) a phase change period where the temperature shows little variation, corresponding to the freezing of a large percentage of the water in the product.
- (3) a cooling period with unsteady state heat transfer where the product is cooled until the required freezing temperature is reached.

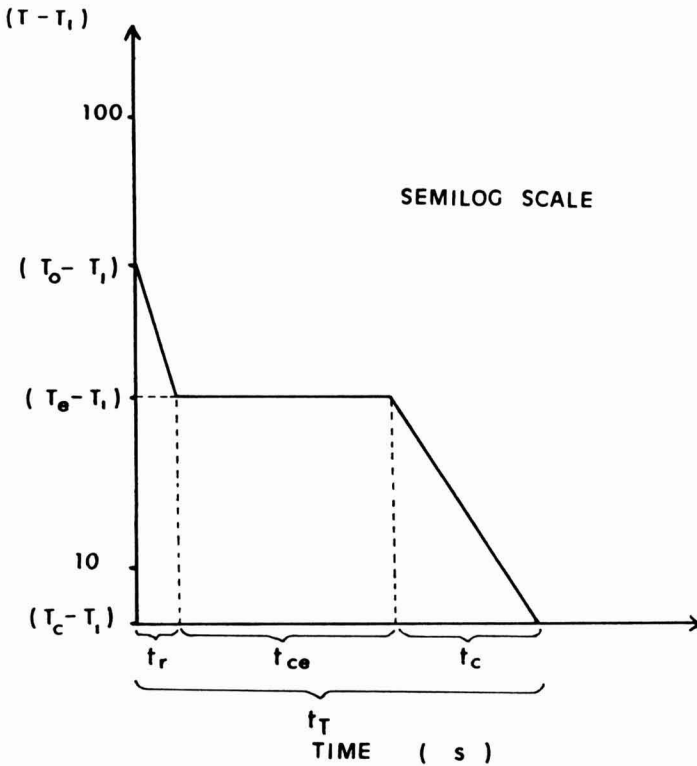


FIG. 1. EXPERIMENTAL FREEZING CURVE (SEMI-LOG REPRESENTATION)

The analytical model proposed in the present study is based on the determination of time corresponding to each of these periods and the total freezing time is the summation of these times:

$$t_T = t_r + t_{ce} + t_c \tag{1}$$

where t_T = total freezing time or time required for the product center to cool from the initial temperature T_o to the desired final freezing temperature T_c .

t_r = precooling time or time required to cool the product at the location $x/L = 0.5$, from its initial temperature T_o to the temperature at the beginning of freezing T_e . The location corresponding to $x/L = 0.5$ (curve 1 in Fig. 2) has been chosen so as to approximately compensate for the excess of heat removed from points $x/L > 0.5$ with the heat still to be removed from $x/L < 0.5$ for infinite cylinders and spheres (Mascheroni and Calvelo 1982). For infinite slabs, Lacroix and Castaigne (1987a) suggested to consider $x/L = 0.4$.

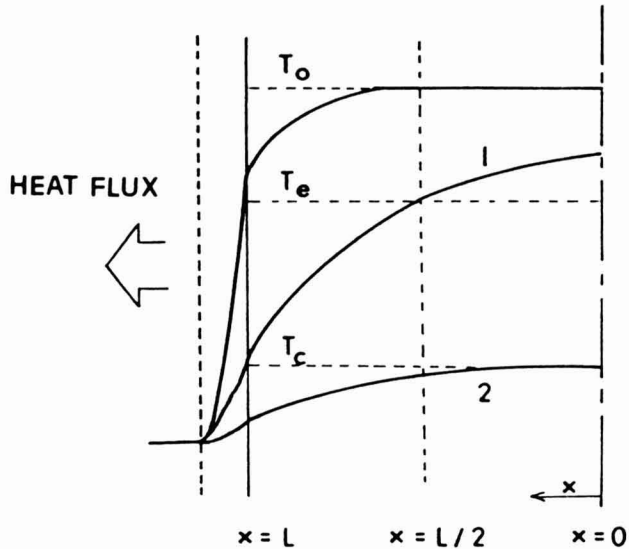


FIG. 2. TEMPERATURE PROFILES AT THE END OF THE PRECOOLING (CURVE 1) AND TEMPERING PERIODS (CURVE 2)

t_{ce} = phase change time at temperature T_e

t_c = tempering time or time required to cool the product center from temperature T_e to the final freezing temperature T_c (curve 2 in Fig. 2).

Ball and Olson (1957) and Pflug *et al.* (1965) showed that the time t required to cool a food product can be expressed by the following equation:

$$t = f \cdot \log \left[j \left(\frac{T_1 - T_i}{T_1 - T} \right) \right] \quad (2)$$

When $F_0 > 0.15$ (which is always the case in freezing calculations)

f = time required to go through a log cycle on the heat penetration curve (Fig. 3); function of Biot number and product thickness.

j = origin ordinate of the heat penetration curve, function of Biot number and location in the product and therefore ratio x/L

t = time

L = half thickness of the slab or half diameter of the cylinder or the sphere

T_i = initial temperature

T_1 = cooling agent temperature

T = product temperature at the position x/L

x = space coordinate (measured from the center of the product)

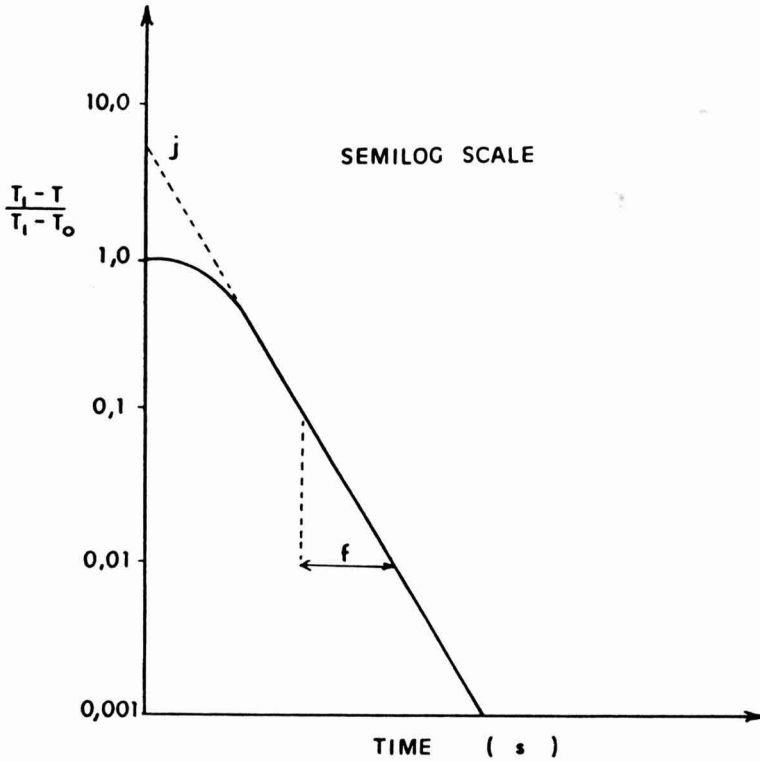


FIG. 3. HEAT PENETRATION CURVE DURING COOLING OF A FOOD PRODUCT

Plank (1941) defined the following equation for the calculation of the change of phase time:

$$\tau_{ce} = \frac{\rho \cdot n_c \cdot E \cdot \lambda \cdot \bar{w} \cdot D^2}{(T_e - T_1) \cdot K_c} \cdot \left(\frac{P}{2 \cdot Bi_c} + R \right) \quad (3)$$

Where: E = water fraction of the unfrozen product

λ = heat of crystallization of pure water at 0°C

w = average of ice fractions at temperatures $\frac{T_1}{w}$ (w_1) and T_c (w_2)

$$= \frac{(w_1 + w_2)}{2} \quad (4)$$

P and R are constants dependant on the geometrical shape of the product.

DESCRIPTION OF THE METHOD

Estimation of the Precooling Time t_r

For this calculation Eq. (2) is used with the following parameters:
 $t = t_r$, $T_i = T_o$, $T = T_e$, $j = j_r$, $f = f_r$. This results in Eq. (5):

$$t_r = f_r \cdot \log \left[j_r \cdot \left(\frac{T_1 - T_e}{T_1 - T_o} \right) \right] \quad (5)$$

where j_r is the j value at the position $x/L = 0.4$ for infinite flat slabs or $x/L = 0.5$ for infinite cylinders and spheres. j_r and f_r are function of Biot number, expressed in this case by:

$$Bi_r = \frac{h \cdot L}{K_r} \quad (6)$$

$$K_r = \frac{K_{nc} + K_c}{2} \quad (7)$$

j_r and f_r . α_r / L^2 values for slabs, infinite cylinders and spheres are given respectively, in Tables 1, 2 and 3 for Biot number $Bi_r > 0.1$. f_r can be calculated from $f_r \alpha_r / L^2$ using:

$$\alpha_r = \frac{\alpha_{nc} + \alpha_c}{2} \quad (8)$$

when $Bi < 0.1$, $j_r = 1$ and $f_r \cdot \alpha_r / L^2 = \text{Ln } 10 / a \cdot Bi$ (9)

where $a = 1$ for an infinite slab
 $a = 2$ for an infinite cylinder
 $a = 3$ for a sphere

An average thermal conductivity K_r and diffusivity α_r is used since during this precooling period, the system behaves with properties of the unfrozen product in the central region and with those of the frozen food with temperatures varying from T_e to values approximating T_1 near the border (Masheroni and Calvelo 1982).

K_{nc} , α_{nc} , K_c , α_c are respectively, the thermal conductivity and diffusivity of the unfrozen product and those of the frozen product at an average temperature $(T_e + T_1)/2$.

Estimation of the Tempering Time t_c

For this calculation, Eq. (2) is used with the following parameters:

TABLE 1.

j_{cc} , j_r , ($f_c \alpha / L^2$) VALUES RELATING TO BIOT NUMBERS FOR AN INFINITE SLAB

Bi	u	j_c	$j_{0.4}$	$f_c \alpha / L^2$
0.1	0.31122	1.01611	1.00825	23.77336
0.2	0.43254	1.03105	1.01565	12.30709
0.3	0.52104	1.04492	1.02231	8.48162
0.4	0.59291	1.05798	1.02836	6.54984
0.5	0.65348	1.07017	1.03382	5.39202
0.6	0.70567	1.08151	1.03871	4.62398
0.7	0.75137	1.09204	1.04309	4.07857
0.8	0.79190	1.10181	1.04699	3.67180
0.9	0.82819	1.11087	1.05047	3.35701
1.0	0.86097	1.11930	1.05358	3.10626
1.2	0.91805	1.13443	1.05880	2.73203
1.4	0.96627	1.14759	1.06293	2.46614
1.6	1.00771	1.15909	1.06620	2.26747
1.8	1.04381	1.16919	1.06875	2.11336
2.0	1.07559	1.17810	1.07073	1.99032
2.5	1.14076	1.19622	1.07383	1.76940
3.0	1.19125	1.20990	1.07513	1.62259
3.5	1.23156	1.22044	1.07532	1.51811
4.0	1.26447	1.22868	1.07484	1.44012
4.5	1.29180	1.23521	1.07395	1.37983
5.0	1.31480	1.24046	1.07283	1.33197
6.0	1.35120	1.24822	1.07030	1.26118
7.0	1.37843	1.25351	1.06775	1.21183
8.0	1.39931	1.25724	1.06539	1.17594
9.0	1.41561	1.25993	1.06328	1.14902
10.0	1.42851	1.26191	1.06145	1.12837
12.0	1.44713	1.26453	1.05852	1.09951
14.0	1.45937	1.26609	1.05642	1.08115
16.0	1.46754	1.26705	1.05494	1.06914
18.0	1.47303	1.26766	1.05391	1.06118
20.0	1.47673	1.26806	1.05319	1.05588
25.0	1.48143	1.26854	1.05227	1.04919
30.0	1.48310	1.26871	1.05193	1.04683
35.0	1.48388	1.26879	1.05177	1.04572
40.0	1.48478	1.26887	1.05159	1.04446
45.0	1.48624	1.26902	1.05129	1.04241
50.0	1.48848	1.26923	1.05083	1.03927
60.0	1.49555	1.26987	1.04934	1.02947
70.0	1.50603	1.27072	1.04703	1.01520
80.0	1.51960	1.27164	1.04387	0.99714
90.0	1.53589	1.27249	1.03980	0.97610
100.0	1.55454	1.27307	1.03478	0.95282
200.0	1.56298	1.27320	1.03238	0.94256
∞	1.57080	1.27324	1.03007	0.93320

$$t = t_c, T_i = T_e, T = T_c, j_c = j_{cc} \text{ and } f = f_c$$

This result in Eq. (10):

$$t_c = f_c \cdot \log \left[j_{cc} \left(\frac{T_1 - T_e}{T_c - T_e} \right) \right] \tag{10}$$

where j_{cc} is the j value for the product center. j_{cc} and $f_c \cdot \alpha c / L^2$ values for slabs, infinite cylinders and spheres are given respectively, in Tables 1, 2 and 3 for Biot number $Bi_c > 0.1$ with

TABLE 2.
 j_{cc} , j_r AND $(f.\alpha/L^2)$ VALUES RELATING TO BIOT NUMBERS FOR
 AN INFINITE CYLINDER

Bi	j_{cc}	j_r	$f.\alpha/L^2$
0,1	1,02437	1,01212	11,80701
0,2	1,04839	1,02355	6,03840
0,3	1,07074	1,03399	4,15640
0,4	1,09265	1,04394	3,19175
0,5	1,11393	1,05333	2,60896
0,6	1,13442	1,06210	2,22121
0,7	1,15405	1,07026	1,94578
0,8	1,17280	1,07782	1,74060
0,9	1,19067	1,08480	1,58211
1,0	1,20767	1,09123	1,45615
1,2	1,23922	1,10260	1,26881
1,4	1,26774	1,11220	1,13633
1,6	1,29351	1,12026	1,03779
1,8	1,31684	1,12703	0,96166
2,0	1,33798	1,13268	0,90110
2,5	1,38269	1,14290	0,79294
3,0	1,41807	1,14903	0,72154
3,5	1,44633	1,15236	0,67098
4,0	1,46909	1,15379	0,63339
4,5	1,48759	1,15394	0,60443
5,0	1,50274	1,15323	0,58151
6,0	1,52560	1,15032	0,54771
7,0	1,54155	1,14654	0,52424
8,0	1,55293	1,14260	0,50721
9,0	1,56122	1,13885	0,49447
10,0	1,56737	1,13545	0,48472
12,0	1,57552	1,12980	0,47114
14,0	1,58036	1,12562	0,46255
16,0	1,58334	1,12262	0,45698
18,0	1,58522	1,12054	0,45333
20,0	1,58641	1,11911	0,45094
25,0	1,58779	1,11735	0,44809
30,0	1,58816	1,11686	0,44731
35,0	1,58824	1,11765	0,44712
40,0	1,58836	1,11658	0,44687
45,0	1,58866	1,11617	0,44623
50,0	1,58920	1,11541	0,44507
60,0	1,59101	1,11267	0,44100
70,0	1,59359	1,10814	0,43474
80,0	1,59650	1,10168	0,42660
90,0	1,59919	1,09310	0,41699
100,0	1,60106	1,08221	0,40627
∞	1,60153	1,07292	0,39818

TABLE 3.

jcc, jr AND $(f.\alpha/L^2)$ VALUES RELATING TO BIOT NUMBERS FOR A SPHERE

Bi	jcc	jr	$f.\alpha/L^2$
0,1	1,02974	1,01719	7,84470
0,2	1,05947	1,03407	3,97288
0,3	1,08723	1,04955	2,73945
0,4	1,11517	1,06487	2,09775
0,5	1,14306	1,07988	1,70665
0,6	1,17060	1,09444	1,44542
0,7	1,19761	1,10845	1,25963
0,8	1,22394	1,12187	1,12125
0,9	1,24954	1,13467	1,01447
1,0	1,27435	1,14686	0,92973
1,2	1,32157	1,16942	0,80400
1,4	1,36560	1,18968	0,71539
1,6	1,40653	1,20783	0,64970
1,8	1,44453	1,22406	0,59910
2,0	1,47978	1,23855	0,55896
2,5	1,55705	1,26824	0,48754
3,0	1,62101	1,29039	0,44061
3,5	1,67404	1,30682	0,40748
4,0	1,71814	1,31888	0,38292
4,5	1,75493	1,32764	0,36403
5,0	1,78575	1,33388	0,34909
6,0	1,83354	1,34112	0,32709
7,0	1,86786	1,34392	0,31181
8,0	1,89289	1,34422	0,30072
9,0	1,91143	1,34319	0,29241
10,0	1,92534	1,34149	0,28603
12,0	1,94405	1,33751	0,27710
14,0	1,95530	1,33381	0,27140
16,0	1,96231	1,33082	0,26767
18,0	1,96676	1,32857	0,26519
20,0	1,96963	1,32694	0,26354
25,0	1,97305	1,32478	0,26150
30,0	1,97403	1,32411	0,26089
35,0	1,97424	1,32397	0,26077
40,0	1,97439	1,32386	0,26067
45,0	1,97484	1,32354	0,26040
50,0	1,97574	1,32289	0,25983
60,0	1,97902	1,32032	0,25772
70,0	1,98394	1,31574	0,25430
80,0	1,98968	1,30874	0,24975
90,0	1,99514	1,29885	0,24428
100,0	1,99901	1,28548	0,23811
∞	2,00000	1,27324	0,23330

$$Bi_c = \frac{h \cdot L}{K_c} \quad (11)$$

$$\text{When } Bi < 0.1, j_c = 1 \text{ and } f_c \cdot \alpha_c/L^2 = \text{Ln}10/a. Bi \quad (12)$$

with $a = 1$ for an infinite slab
 $a = 2$ for an infinite cylinder
 $a = 3$ for a sphere

The property values to be used are those of the frozen product evaluated at the average temperature $(T_1 + T_e)/2$ since the temperature profile is not flat when $Bi > 0.1$ (Fig. 2, curve 2).

Estimation of t_r and t_c for Rectangular Parallelepipeds (Bricks) and Finite Cylinders

In the case of rectangular bricks, Eq. (5) and (10) can be used to estimate t_r and t_c . The f_r, j_r, f_c and j_{cc} values to be considered in these equations are obtained by applying Newman's rule (Chapman 1967; Carslaw and Jaeger 1957):

$$\frac{1}{f_r} = \frac{1}{f_{r1}} + \frac{1}{f_{r2}} + \frac{1}{f_{r3}} \quad (13)$$

$$\frac{1}{f_c} = \frac{1}{f_{c1}} + \frac{1}{f_{c2}} + \frac{1}{f_{c3}} \quad (14)$$

$$j_r = j_{r1} \cdot j_{r2} \cdot j_{r3} \quad (15)$$

$$j_{cc} = j_{cc1} \cdot j_{cc2} \cdot j_{cc3} \quad (16)$$

where, f_{r1}, j_{r1}, f_{c1} and j_{cc1} are the values calculated for a slab of thickness equal to the length of the brick.

f_{r2}, j_{r2}, f_{c2} and j_{cc2} are the values calculated for a slab of thickness equal to the width of the brick.

f_{r3}, j_{r3}, f_{c3} and j_{cc3} are the values obtained for a slab of thickness equal to the height of the brick.

In the same way, f_r, j_r, f_c and j_{cc} values to be used in Eq. (5) and (10) for a finite cylinder are:

$$\frac{1}{f_r} = \frac{1}{f_{r1}} + \frac{1}{f_{r2}} \quad (17)$$

$$\frac{1}{f_c} = \frac{1}{f_{c1}} + \frac{1}{f_{c2}} \quad (18)$$

$$j_r = j_{r1} \cdot j_{r2} \quad (19)$$

$$j_{cc} = j_{cc1} \cdot j_{cc2} \quad (20)$$

where f_{r1} j_{r1} f_{c1} j_{cc1} are the calculated values for a slab of thickness equal to the length of the finite cylinder.

f_{r2} , j_{r2} , f_{c2} , j_{cc2} are the calculated values for an infinite cylinder of diameter equal to the diameter of the finite cylinder.

Calculation of Phase Change Time

For the change of phase period, an equation similar to the original Plank's Eq. (3) (Plank 1941) is used :

$$t_{ce} = \frac{\rho_{nc} \cdot E \cdot \lambda \cdot \bar{w} \cdot D^2}{(T_e - T_1) \cdot K_c} \left[\frac{P_1}{2 \cdot B_1^2} + R_1 \right] \quad (21)$$

P_1 and R_1 are constants dependant on the geometrical shape of the product. P_1 and R_1 to use in Eq. (21) have been determined by Lacroix and Castaigne (1987a and b):

for slabs $P_1 = 0.51233$
 $R_1 = 0.15396$

for infinite cylinders $P_1 = 0.27553$
 $R_1 = 0.07212$

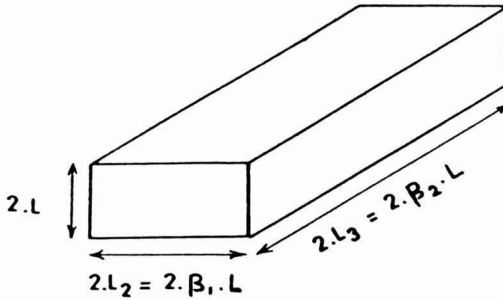
for spheres $P_1 = 0.19665$
 $R_1 = 0.03939$

for bricks of dimensions $2L$, $2\beta_1 \cdot L$, $2\beta_2 \cdot L$ (assuming $2L$ to be the smallest side of the brick as in Fig. 4), P_1 and R_1 are given by the following equations:

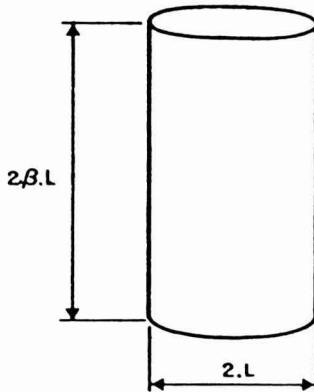
$$P_1 = P \left[-0.02175 \cdot \frac{1}{(\beta \bar{T})_c} - 0.01956 \cdot \frac{1}{\bar{S}te} - 1.69657 \right] \quad (22)$$

$$R_1 = R \left[5.57519 \cdot \frac{1}{(\beta \bar{T})_c} + 0.02932 \cdot \frac{1}{\bar{S}te} + 1.58247 \right] \quad (23)$$

where P and R are Plank's constants given by Ede's charts or in Tables 4 and 5 (Castaigne and Lacroix 1985).



A



B

FIG. 4. CHARACTERISTIC DIMENSIONS FOR A RECTANGULAR PARALLELEPIPED (A) AND FOR A FINITE CYLINDER (B)

for finite cylinders of dimensions $2L$, $2\beta_2 \cdot L$ (assuming $2L$ to be the diameter of the cylinder) (Fig. 4), P_1 and R_1 can be obtained from Tables 4 and 5, considering $\beta_1 = 1$. If $\beta_2 < 1$, P_1 and R_1 values for $\beta_2 = \beta_1 = 1$ are used in Eq. (21).

TABLE 4.
P VALUES RELATING TO β_1 AND β_2 VALUES ($\times 10^3$)
(from Castaigne and Lacroix 1985)

β_1	1.0	1.1	1.2	1.3	1.4	1.5	1.6	1.7	1.8	1.9	2.0	2.5	3.0	3.5	4.0	4.5	5.0	6.0	7.0	8.0	9.0	10.0	∞		
1.0	167																								
1.1	172	177																							
1.2	176	182	188																						
1.3	181	187	192	197																					
1.4	184	191	196	201	206																				
1.5	188	194	200	205	210	214																			
1.6	190	197	203	209	214	218	222																		
1.7	193	200	206	212	217	222	226	230																	
1.8	196	203	209	215	220	225	229	233	237																
1.9	198	205	212	218	223	228	232	236	240	244															
2.0	200	208	214	220	226	231	235	239	243	247	250														
2.5	208	217	224	230	236	242	247	251	256	260	263	278													
3.0	214	223	231	238	244	250	255	260	265	269	273	288	300												
3.5	219	228	236	243	250	256	262	267	272	276	280	297	309	318											
4.0	222	232	240	248	255	261	267	272	277	281	286	303	316	326	333										
4.5	225	235	243	251	258	265	271	276	281	286	290	308	321	332	340	349									
5.0	227	237	246	254	261	268	274	280	285	290	294	313	326	337	345	352	357								
6.0	231	241	250	258	266	273	279	285	290	295	300	319	333	344	353	360	366	375							
7.0	233	244	253	261	269	276	283	289	294	300	304	324	339	350	359	366	372	382	389						
8.0	235	246	255	264	272	279	286	292	298	303	308	328	343	354	364	371	377	387	394	400					
9.0	237	248	257	266	274	281	288	294	300	305	310	331	346	358	367	375	381	391	399	404	409				
10.0	238	249	259	267	276	283	290	296	302	307	313	333	349	361	367	378	385	395	402	408	413	417			
∞	250	262	273	283	292	300	308	315	321	328	333	357	375	389	400	409	417	429	437	444	450	455	500		

TABLE 5.
R VALUES RELATING TO β_1 AND β_2 VALUES ($\times 10^3$)
(from Castaigne and Lacroix 1985)

β_1	1.0	1.1	1.2	1.3	1.4	1.5	1.6	1.7	1.8	1.9	2.0	2.5	3.0	3.5	4.0	4.5	5.0	6.0	7.0	8.0	9.0	10.0	∞		
1.0	42																								
1.1	44	47																							
1.2	46	49	51																						
1.3	47	50	52	54																					
1.4	48	51	54	56	58																				
1.5	49	53	55	57	59	60																			
1.6	50	54	56	58	60	62	63																		
1.7	51	54	57	59	61	63	64	65																	
1.8	51	55	58	60	62	64	65	67	68																
1.9	52	56	59	61	63	65	66	67	69	70															
2.0	52	56	59	62	64	66	67	68	70	71	72														
2.5	54	59	62	64	67	69	70	72	73	74	75	79													
3.0	56	60	63	66	69	71	72	74	75	77	78	82	85												
3.5	57	61	65	68	70	72	74	76	77	78	79	84	87	89											
4.0	57	62	66	69	71	73	75	77	78	80	81	85	89	91	93										
4.5	58	63	66	69	72	74	76	78	79	81	82	87	90	92	94	96									
5.0	58	63	67	70	72	75	77	78	80	81	83	88	91	93	95	97	98								
6.0	59	64	68	71	73	76	78	80	81	83	84	89	93	95	97	99	100	102							
7.0	60	64	68	71	74	77	79	80	82	84	85	90	94	96	98	100	101	103	105						
8.0	60	65	69	72	75	77	79	81	83	84	86	91	95	97	99	101	102	104	106	107					
9.0	60	65	69	72	75	78	80	82	83	85	86	92	95	98	100	102	103	105	107	108	109				
0.0	60	65	69	73	75	78	80	82	84	85	87	92	96	99	100	102	104	106	107	108	109	110			
∞	63	67	72	75	78	81	83	86	87	88	91	97	102	103	106	108	110	113	115	115	116	117	125		

It can be noticed that when β_1 , or β_2 is higher than 10, the product shape will be assumed infinite.

The freezing point for most materials is not sharp, since latent heat release and the change in thermal conductivity take place over a range of temperature. To take this into account, Pham (1984) defined a "mean freezing temperature" which is found to be approximately 1.5 K below the initial freezing temperature for Tylose, meat and similar material. This temperature is to be used in the calculations as temperature T_e (change of phase temperature).

TESTING OF THE MODEL

Testing of the model was carried out by comparing numerical experimental datas obtained from the literature for different geometrical shaped food products. Datas on Karlshrue test substance (tylose) were taken from Cleland and Earle (1977) for infinite flat slabs (43 experiments), from Cleland and Earle (1979a) for infinite cylinders (30 experiments) and spheres (30 experiments). Data on Tylose and meat were taken from Cleland and Earle (1979b) (72 experiments) and De Michelis and Calvelo (1983) (19 experiments) for rectangular bricks and from De Michelis and Calvelo (1983) (4 experiments on meat) for finite cylinders. These experiments cover a wide range of conditions that are commonly found in food freezers. They provide a database of 194 experiments for two materials, with two final temperatures, a variety of regular geometries and wide variations of Biot number, initial temperature and cooling medium temperature (Table 6). More details on the data used to test the model can be obtained from Lacroix and Castaigne (1987a and b).

The deviations between the experimental freezing times and the corresponding calculated times were expressed as a % error (percentage difference between experimental and predicted freezing times). The model gives very good agreement with data for all the shapes tested (Table 7): the means of % errors are closed to zero and the standard deviations are very low for this type of calculations. From Table 6, it can be concluded that this method is equivalent in terms of accuracy for the various infinite and finite shapes tested with a reliable finite differences method.

A systematic assessment of major freezing time prediction methods has been carried out by Cleland and Earle (1984). This paper includes numerical methods (finite differences methods) as well as simple formula (Pham 1984; Hung and Thompson 1983; De Michelis and Calvelo 1983; Cleland and Earle 1982). Table 8 summarizes in general terms the performance of these four analytical methods and the method exposed in the present paper. It appears from Tables 7 and 8 that our method works satisfactorily compared to the various methods tested, including regression formula and finite differences computations. Moreover, Table 9 shows that Lacroix and Castaigne's model performs equally well under the

TABLE 6.
RANGE OF CONDITIONS COVERED BY THE EXPERIMENTAL DATA
USED TO TEST THE MODEL

Shape	Data number	Dimensions $2l$ (m)	Cooling medium temperature T_f ($^{\circ}\text{C}$)	Initial temperature T_o ($^{\circ}\text{C}$)	Final freezing temperature T_c ($^{\circ}\text{C}$)	Heat transfer coefficient ($\text{W/m}^2 \cdot ^{\circ}\text{C}$)	B_{tr}	Bi_c	Experimental freezing time (h)
Infinite flat slab	43	0.025 - 0.10 m	-40, -20 $^{\circ}\text{C}$	3, 35 $^{\circ}\text{C}$	-10 $^{\circ}\text{C}$	10 - 500	0.15 - 14.5	0.10 - 9.7	0.32 - 8.96
Infinite cylinder	30	0.05 - 0.15 m	-40, -20 $^{\circ}\text{C}$	4, 30 $^{\circ}\text{C}$	-10 $^{\circ}\text{C}$	18 - 37	0.56 - 2.54	0.37 - 1.67	1.04 - 9.36
Sphere	30	0.05 - 0.16 m	-40, -20 $^{\circ}\text{C}$	1, 30 $^{\circ}\text{C}$	-10 $^{\circ}\text{C}$	27 - 53	0.66 - 3.29	0.44 - 2.19	0.66 - 5.24
Rectangular parallelepiped	91	0.062 - 0.103 m	-45, -15 $^{\circ}\text{C}$	1.9, 30 $^{\circ}\text{C}$	-10 or -18 $^{\circ}\text{C}$	20 - 260	0.33 - 16.0	0.22 - 10.7	0.62 - 9.08
		$1 \leq \beta_1 \leq 4$ $1 \leq \beta_2 \leq \infty$					0.33 - 28.0	0.22 - 18.7	
Finite cylinder	4	0.044 - 0.076 m	-40, -44 $^{\circ}\text{C}$	3.5, 22 $^{\circ}\text{C}$	-18 $^{\circ}\text{C}$	28 - 40	0.51 - ∞	0.34 - ∞	0.62 - 1.32
		$0.72 \leq \beta_2 \leq 1.65$					0.83 - 1.30	0.55 - 0.86	0.62 - 1.32
							0.89 - 2.14	0.59 - 1.42	

TABLE 7.
RESULTS FROM COMPARISONS OF EXPERIMENTAL WITH THE PREDICTED
FREEZING TIMES, BASED ON PUBLISHED DATAPOINTS

	Method developed in this paper				Finite differences method (Cleland and Earle, 1984)		
	Mean of % error (a)	Standard deviation of % error	90% confidence interval about the mean	Mean of % error	Standard deviation of % error	90% confidence interval about the mean	
Infinite flat slabs (1)	-0.72	3.63	- 6.8, + 5.4	0.0	5.3	- 8.9, + 8.9	
Infinite cylinders (2)	-0.19	5.28	- 9.2, + 8.8	-1.8	5.2	-10.6, + 7.0	
Spheres (3)	-0.38	4.45	- 7.9, + 7.2	-0.3	3.3	- 5.9, + 5.3	
Rectangular bricks (4)	-1.27	7.15	-13.2, + 10.6	-0.7 (6)	14.3 (6)	-24.4, + 23.1 (6)	
Finite cylinders (5)	1.02	4.58	- 9.8, + 11.8	-	-	-	

(a) Ratio of the difference between experimental and predicted freezing times on experimental freezing time.

- (1) based on Cleland and Earle's (1977) 43 datapoints
- (2) based on Cleland and Earle's (1979a) 30 datapoints
- (3) based on Cleland and Earle's (1979b) 30 datapoints
- (4) based on Cleland and Earle's (1979c) 72 datapoints (For Tylose) and De Michelis and Calvelo (1983) 19 datapoints (for meat)
- (5) based on De Michelis and Calvelo's (1983) 4 datapoints for meat
- (6) based on (4) and (5) together

TABLE 8.
PERFORMANCE OF VARIOUS METHODS FOR PREDICTING FREEZING TIMES

Method	Mean of % error	Standard deviation of % error	% error range	90% confidence interval about the mean
Cleland and Earle (1982) ¹	-2.4	8.5	-30, + 23	-16.4, + 11.6
Pham (1984) ¹	0.3	6.7	-24, + 18	-10.7, + 11.3
Hung and Thompson (1983) ¹	12.5	11.8	-17, + 44	- 6.9, + 31.9
De Michelis and Calvelo (1983) ¹	-8.7	15.1	-48, + 38	-33.5, + 16.1
Lacroix and Castaigne (this paper) ²	0.80	5.85	-16.3, + 14.7	- 8.8, + 10.4

¹Results from Cleland and Earle (1984) based on 275 datapoints

²Based on the 198 datapoints of this paper

TABLE 9.
EVALUATION OF THE METHOD FOR VARIOUS INTERVALS OF
EXPERIMENTAL CONDITIONS FOR THE 198 DATAPOINTS

Parameter under consideration	Range	Number of experiments	Mean of % error	Standard deviation of % error	90% confidence interval about the mean
Biot number Bi	< 4.0 ≥ 4.0	173 25	- 0.69 - 1.54	5.61 7.25	-10.0, + 8.6 -14.3, + 11.3
Heat transfer coefficient h	$< 60 \text{ W/m}^2 \cdot \text{C}$ $\geq 60 \text{ W/m}^2 \cdot \text{C}$	142 56	+ 0.10 - 3.08	4.95 7.18	- 8.1, + 8.3 -15.1, + 8.9
Initial temperature T_o	$To < 10^\circ\text{C}$ $10^\circ\text{C} \leq To < 20^\circ\text{C}$ $To \geq 20^\circ\text{C}$	61 65 72	- 3.02 - 2.02 + 2.18	5.85 5.38 4.96	-12.8, + 6.8 -11.0, + 7.0 - 6.1, + 10.5
Final freezing temperature T_f	$T_f = -10^\circ\text{C}$ $T_f = -18^\circ\text{C}$	192 6	- 0.88 + 1.77	5.89 3.41	-10.6, + 8.8 - 5.2, + 8.7
Cooling medium temperature T_1	$T_1 \geq -25^\circ\text{C}$ $T_1 < -25^\circ\text{C}$	84 114	- 1.71 - 0.13	4.89 6.38	- 9.8, + 6.4 -10.7, + 10.5

¹For parallelepipeds and finite cylinders, Bi is the Biot number for the smallest side of the shape

various experimental set of conditions used in the present study. Inaccuracy is always less than 15% and more often less than 10% in all the cases, even in extreme situations. Cleland and Earle (1984) discussed the strengths and the weaknesses of the four recent analytical prediction methods tested in their study. Each of them has a specific range of experimental conditions where it allows reliable prediction but it is not equally accurate over the whole data set. Differences between experimental and predicted freezing times are sometimes very high. For example, Cleland and Earle's method involved errors as high as 30% for a final center temperature equal to -18°C . The Hung and Thompson method showed reverse trends with a poor fit to -10°C final center temperature. The method of Pham gave the most consistent results over the whole data set and the method of De Michelis and Calvelo apparently performed worse than the others in terms of spread. It appears in Table 9 that the accuracy of Lacroix and Castaigne's method is almost not affected by Biot number, heat transfer coefficient, initial and final center temperatures and cooling medium temperature values over the wide range of experimental conditions used in the present study.

CONCLUSIONS

The method presented in this paper has the following advantages:

allows simple and fast calculations of freezing time for a variety of simple geometrical shaped products;

is based on heat transfer principles rather than on empirical corrections;

requires no use of graphs, empirical constants or advanced algebra;

yields values for the precooling, freezing and subcooling times separately;

agrees with experimental data as well as or better than any other previous method, including finite difference computations, for the wide range of experimental conditions used;

is equally accurate over the wide range of conditions tested;

allows calculations for different initial temperatures and various final temperatures at the thermal center;

is easily programmable in scientific calculators (such as HP41C) or microcomputers (programs for HP41C are available from the authors upon request).

An example of freezing time calculation for french fries is detailed in Annex 1.

ACKNOWLEDGMENTS

The authors gratefully acknowledge the financial support form CRSAQ (Conseil des recherches et services agricoles du Quebec).

LIST OF SYMBOLS:

- \overline{Bi} — Biot number (hL/K)
 C_p — Specific heat ($J/Kg \text{ } ^\circ C$)
 E — Water fraction in the product
 f — Time required to go through one log cycle on the heat penetration curve (s) (Fig. 3)
 F_o — Fourier number $\alpha.t/L^2$
 h — Heat transfer coefficient ($W/m^2 \text{ } ^\circ C$)
 j — Origin ordinate on the heat penetration cruve (Fig. 3)
 $j_{x/L}$ — j value at the position x/L
 K — Thermal conductivity ($W/,K$)
 L — Half thickness of the slab, half diameter of the cylinder or of the sphere (m)
 Ste — Stephan number ($\rho c. C_{pc}. (T_e - T_1)/\rho_{nc}. E. \lambda. w$)
 t — Time (s)
 T — Product temperature at the position x/L ($^\circ C$ or K)
 T_c — Final temperature at the center of the frozen product
 T_e — Temperature for beginning of freezing
 T_i — Product initial temperature of the non-stationary periods
 T_1 — Coolant temperature
 T_o — Product temperature at $t = 0$
 X — Space coordinate measured from the product center (m)
 α — Thermal diffusivity (m^2/s), $\alpha = K/\rho.C^p$
 ρ — Density of the product (kg/m^3)
 λ — Heat of crystallization of pure water at $0^\circ C$ (J/kg)
 \overline{w} — Average ice content of the product at T_c (W_1) and T_1 (W_2)

$$\overline{W} = \frac{W_1 + W_2}{2}$$

Indices r, c and nc indicate values of the considered variable for respectively, precooling period, tempering period (or frozen product at temperature $(T_c + T_1)/2$) and unfrozen product.

REFERENCES

- BALL, C. W. and OLSON, F. C. W. 1957. *Sterilisation in Food Technology*, pp. 654, McGraw Hill, New York.
- CARSLAW, H. S. and JAEGER, J. C. 1959. *Conduction of Heat in Solids*. Oxford University Press, New York.
- CASTAIGNE, F. and LACROIX, C. 1985. Methode simple permettant d'estimer les temps de congelation de produits ayant des formes simples. *Revue generale du Froid*, 74, 251.
- CHAPMAN, A. J. 1967. *Heat Transfer*. MacMillan Co., New York.
- CLELAND, A. C. and EARLE, R. L. 1977. A comparison of analytical and numerical methods for predicting the freezing times of foods. *J. Food Sci.* 42, 1390.
- CLELAND, A. C. and EARLE, R. L. 1979a. A comparison of methods for predicting the freezing times of cylindrical and spherical foodstuffs. *J. Food Sci.* 44, 958.
- CLELAND, A. C. and EARLE, R. L. 1979b. Prediction of freezing times for foods in rectangular packages. *J. Food Sci.* 44, 964.
- CLELAND, A. C. and EARLE, R. L. 1982. A simple method for prediction of heating and cooling rates in solids of various shapes. *Revue Internationale du Froid*, 5, 98.
- CLELAND, A. C. and EARLE, R. L. 1984. Assessment of freezing time predictions. *J. Food Sci.* 49, 1034.
- DE MICHELIS, A. and CALVELO, A. 1982. Mathematical models for symmetric freezing of beef. *J. Food Sci.* 47, 1211.
- DE MICHELIS, A. and CALVELO, A. 1983. Freezing time predictions for brick and cylindrical shaped foods. *J. Food Sci.* 48, 909.
- HUNG, Y. C. and THOMPSON, D. R. 1983. Freezing time prediction for slab shape foodstuffs by an improved analytical method. *J. Food Sci.* 48, 555.
- LACROIX, C. and CASTAIGNE, F. 1987a. Simple method for freezing time calculations for infinite flat slabs, infinite cylinders and spheres. *Can. Inst. Food Sci. Technol. J.* 20, 252.
- LACROIX, C. and CASTAIGNE, F. 1987b. Simple method for freezing time calculations for brick and cylindrical shaped food products. *Can Inst. Food Sci. Technol. J.* 20, 342.
- MASCHERONI, R. H. and CALVELO, A. 1982. A simplified model for freezing time calculations in foods. *J. Food Sci.* 47, 1201.
- NAGAOKA, J., TAKAJI, S. and HOHANI, S. 1955. Experiments on the freezing of fish in air blast freezer, *Proc. IX Int. Cong. Refrig.* 4, 105.
- PFLUG, I. J., BLAISDELL, J. L. and KOPOLMAN, I. J. 1965. Developing temperature time curves for objects that can be approximated by a sphere, infinite plate or infinite cylinder - *ASHRAE Trans.* 71, 238.

- PLANK, R. 1941. Beiträge zur Berechnung und Bewertung der Gefriereschwindigkeit von Lebensmitteln, z. ges. Kalteind., 10, Beih Reihe 3, 1.
- PLANK, R. 1963. *El Empleo del Frio en la Industria de la Alimentacion*. Editorial Reverte. Barcelona.
- PHAM, Q. T. 1984. Extension to Plank's equation for predicting freezing times of foodstuffs of simple shapes. *Revue International du Froid*, 7, 377.
- RAMASWAMY, H. S. and TUNG, M. A. 1984. A review of predicting freezing times of foods. *J. Food Proc. Eng.* 7, 169.

ANNEXE I. FREEZING TIME CALCULATION FOR FRENCH FRIES

1—Data

- (a) Dimensions: thickness: 0.010 m
 width: 0.012 m
 length: 0.08 m

(b) Thermophysical data:

Unfrozen Product

$$K_{nc} = 0.45 \text{ W/m.K}$$

$$\varphi_{nc} = 1100 \text{ kg/m}^3$$

$$C_{pnc} = 3800 \text{ J/kg K}$$

$$\alpha_{nc} = 1.077 \times 10^{-7} \text{ m}^2/\text{s}$$

Frozen Product

$$K_c = 1.7 \text{ W/mK}$$

$$\varphi_c = 980 \text{ kg/m}^3$$

$$C_{pc} = 1800 \text{ J/kg K}$$

$$\alpha_c = 9.637 \times 10^{-7} \text{ m}^2/\text{s}$$

(c) Thermal data:

$$\text{Initial temperature } T_0 = 45^\circ\text{C}$$

$$\text{Cooling medium temperature } T_1 = -26^\circ\text{C}$$

$$\text{Mean freezing temperature } T_e = -2.5^\circ\text{C}$$

$$\text{Final freezing temperature (product center) } T_c = -18^\circ\text{C}$$

(d) Others

$$\text{Water content } E = 75\% = 0.75$$

$$\text{Average ice content } \bar{W} = 0.85$$

$$h = 70 \text{ w/m}^2 \text{ K}$$

2—Calculation

(a) Constant values

$$K_r = 1.075 \text{ W/mK}$$

$$\beta_1 = 1.2$$

$$\beta_2 = 8$$

$$\alpha_r = 5.357 \times 10^{-7} \text{ m}^2/\text{s}$$

$$P = 0.255 \text{ (from Tables 4 and 5)}$$

$$R = 0.069$$

(b) Freezing time, calculation

		Thickness 1×10^{-2} m	Width 1.2×10^{-2} m	Length 8×10^{-2} m	Average value
P	Biot number	0.326	0.391	2.605	
R	j_r	1.023	1.028	1.074	1.1295
E	$4 \text{ fr. } \alpha_r / L^2$	8	6.5	1.74	
C	f_r	373	437	5197	194
O	t_r				103 s
O					
L					
I					
N					
G					
T	Biot number	0.206	0.247	1.647	
E	j_c	1.031	1.037	1.160	1.2402
M	$4 \text{ fr. } \alpha_c / L^2$	12.3	10	2.22	
P	f_c	319	374	3685	164.5
E	t_c				92 s
R					
I					
N					
G					
P C	Biot number	0.206			
H H	Stephan number	0.1765			
A A	P_1	-0.488			
S N	R_1	1.988			
E G	t_{ce}				472 s
E					

TOTAL FREEZING TIME = 667 s = 11 min 7 s

THERMAL CONDUCTIVITY OF CONCENTRATED WHOLE MILK

G. R. MORE¹

*Dairy Engineering Division, National Dairy Research Institute,
KARNAL-132001. INDIA*

and

SURESH PRASAD

*Post Harvest Technology Centre
Indian Institute of Technology
KHARAGPUR-721302. INDIA*

Accepted for Publication January 8, 1988

ABSTRACT

The information of thermal conductivity of milk is required for the design of heat exchanger equipment in the dairy processing. Thermal conductivity of whole milk was experimentally determined by a steady-state, parallel disk, relative method at various concentrations (from 37 to 72.4% total solids) and temperature range between 40 to 90°C. This thermal property of milk increased with rise in temperature and decreased with increase in total solids content and its values varied from 0.278 to 0.491 W/m K. An expression has been proposed for derivation of milk thermal conductivity from temperature and total solids content.

INTRODUCTION

Thermal and physical properties of milk are required for adequate design and analysis of the process. Some of these properties may be evaluated readily by simple additive rules, others, such as viscosity and thermal conductivity cannot be predicted with precision. Among the thermal properties, thermal conductivity of milk has received rather little attention from the authors. With few exceptions, most of the data on thermal conductivity of milk and milk products in the past were obtained at low concentration and temperature.

¹Correspondence should be sent to Dr. G. R. More, Scientist, Dairy Engineering Division, National Dairy Research Institute, KARNAL-132001. INDIA

Riedel (1949) measured thermal conductivity of fresh whole milk (3.6% fat), whole milk (2.5% fat) and its concentrates at concentration degree of 1.9 and 2.54 skimmilk, buttermilk and whey at 1.5, 20, 50 and 80°C. Leidenfrost (1959) studied homogenized unsweetened condensed milk (10% fat, 67% water) and its derived samples at concentration degree 0.30, 0.60, 1.52 and at about 20, 40, 60 and 80°C. Konrad and Rabke (1971) made thermal conductivity measurements on skimmilk and its 20, 30 and 40% total solids concentrates, 2.5% fat whole milk and its 7.6% fat 27% solids-not-fat concentrate at about 20 and 60°C. Fernandez-Martin and Montes (1972) have used a steady-state and relative method for determining the thermal conductivity of skimmilk, half-and-half milk, whole milk and their concentrates up to about 30 to 40% total solids, over the temperature range of 5 to 75°C. A nomogram is also presented for the ready derivation of milk thermal conductivity from temperature, total solids content and fat to solids-not-fat ratio. Agrawala and Ojha (1972) also used a steady-state method for determining thermal conductivity of concentrated milk (up to 28% total solids) for a temperature range of 40 to 90°C, whereas Sweat and Parmelle (1978) employed a line heat source conductivity probe for measuring thermal conductivity of condensed milk and evaporated milk over a limited temperature range (0, 20 and 40°C.)

The purpose of this investigation was to determine whole milk thermal conductivity over wide ranges of temperatures and composition and to develop an expression on this behavior for prediction of this thermal property.

MATERIALS AND METHODS

A steady-state, parallel-plate, resistance method was employed for determining the thermal conductivity of whole milk. The design of the thermal conductivity apparatus was based on Bate's (1936) work and a modified unit used by Agrawala and Ojha (1972).

(1) **Sample preparation:** Fresh cow milk from Jersey Bull Mother Dairy Farm of Indian Institute of Technology, Kharagpur was taken for this study. The fat content of the sample was determined by the standard Gerber test and was about 4.1%. The concentrated milk sample for measuring thermal and physical properties was prepared by the traditional method (De and Ray 1952). The total solids content of the sample was determined by Gravimetric method. The prepared sample was allowed to cool down to room temperature before using it for the experiment.

(2) **Apparatus:** The thermal conductivity apparatus was made of two separate parts. The upper part consists of a copper cylinder which encloses an electric heater of 500 watt capacity (Fig. 1). A 6 mm thick circular perspex (Polymethyl

methacrylate) disc was fixed below the heater as a reference material. A uniform temperature all along the top surface of reference disk was achieved by proper fabrication of the heating coil and the further distribution of this heat was made uniform by fixing a 2 mm thick brass disk between the heater and the reference material. A fiber glass insulation was provided at the top of the heater to reduce the radiation losses.

The lower part of the apparatus consists of a bekelite cup of which bottom was closed by a 2 mm brass disk. The upper part sits in the slot of the lower one and makes a space of 11 mm thickness for keeping the sample. This bekelite material acts as an insulation to the sample and the upper part. The cooling brass disk, which provides a surface to the product, was maintained at constant temperature by circulating a large quantity of uniformly distributed water through the channels made at its bottom. The cooling water, maintained at constant temperature in the thermostatically controlled water bath, was circulated through the channels of the apparatus by a centrifugal pump.

This method for the study was chosen because it would not let convection currents develop in the sample under test and moreover, fat separation from the sample during the experiment was minimized by having less thickness of the product and minimum temperature difference between the surfaces. Therefore, even the cooling water was heated to bring down this difference. The heating and cooling plates were designed such that the temperature distribution on the surfaces was uniform. For cooling plate, this was achieved by having channels to guide the incoming and outgoing water side by side and hence reducing temperature difference within cooling water.

For measuring the temperature at different points in the thermal conductivity apparatus, copper-constantan thermocouples were employed. The average temperature at the surface of perspex disk was measured by fixing three thermocouples on each side. Three more thermocouples were fixed on the top surface of the heating coil. Similarly, three thermocouples on each side of the cooling brass disk were also fixed for measuring the average temperature at the bottom surface of the sample and that of the cooling water. In each case, thermocouples were placed 120° apart from the center and with radial distances of 1 cm, 2 cm and 3 cm, respectively. The thermocouple T_1 was connected to a temperature controller for maintaining a constant temperature of the heating coil. The temperature of the heater was varied with the help of voltage control by a variac (rheostat). A digital temperature indicator, calibrated at room temperature, was used for measuring temperature at different points in the apparatus. For quick positioning of the different thermocouples, a selector switch was put in the circuit. More details of the thermal conductivity unit is given by Agrawala and Ojha (1972).

(3) Procedures: First the temperature of water in the waterbath was brought to about 2 to 3 degrees below the average temperature of the sample to be main-

tained and the thermostat was set. The thermal conductivity apparatus was levelled with a level gauge. The sample was put in the sample chamber with a uniform thickness up to the slot of the lower cup. The upper part of the apparatus was put over the sample. Care was taken to avoid any trapping of air bubbles between the sample and the perspex disk. This was achieved by maintaining a proper level of the sample, putting upper part from slanted to horizontal position and by giving little rotation to it. Also during the experiment, the sample was heated to a slightly higher temperature to remove air bubbles present inside the sample. The heating coil temperature was maintained in such a way that the temperature drop across the sample remained about 3°C. It helps to reduce the convection current within the sample. Initially, temperature of the heater was kept higher than the required one in order to reduce the time required to bring the system to steady-state (Mohsenin 1980). The voltage in the heating coil was regulated in such a way that the deviation from its set temperature was minimum. When the sample came to steady-state, which was generally achieved after 4 to 5 h, a constant temperature was observed at least for another 2 h and when it was confirmed that there was no more change in the temperature of the system, the final temperature at each point was recorded.

The water-bath was then set for the next higher temperature and the above mentioned procedure was repeated for different temperatures. Similar method was adopted for finding the thermal conductivity of samples at various concentrations. Thermal conductivity was determined by application of Fourier's law of unidirectional conduction of heat and for steady-state condition it becomes,

$$\frac{\dot{q}}{A} = \frac{K(T_1 - T_2)}{x} \quad (1)$$

Under steady-state condition and if heat losses are negligible, the ratio of the temperature difference across a perspex disk and a layer of the sample is equal to the ratio of their thermal resistances.

$$\frac{\dot{q}}{A} = \frac{K_p(T_1 - T_2)}{x_p} = \frac{K_m(T_2 - T_3)}{x_m}$$

or

$$\begin{aligned} K_m &= \left(\frac{K_p}{x_p/x_m} \right) \left(\frac{T_1 - T_2}{T_2 - T_3} \right) \\ &= A_c \left(\frac{T_1 - T_2}{T_2 - T_3} \right) \end{aligned} \quad (2)$$

For determining the apparatus constant, at a constant temperature, heat from the electrical heater was allowed to flow down through the perspex disk, distilled water layer and away through the cooling water. The apparatus constant was computed by using the following equation,

$$A_c = \frac{K_d(T_2 - T_3)}{(T_1 - T_2)} \quad (3)$$

RESULTS AND DISCUSSION

The thermal conductivity of whole milk was determined at temperature range between 40 and 90°C and at four different concentrations 37, 50, 60, 72% total solids content. The thermal conductivity apparatus was calibrated over the temperature range of 40 to 90°C using glycerol and the values of the apparatus constant are shown in Table 1 and the reproducibility of measurements assessed by thermal conductivity determinations on distilled water. The error was found to be within -1.38%.

TABLE 1.
APPARATUS CONSTANT (A_c) FOR DETERMINATION OF
THERMAL CONDUCTIVITY

Average Temperature of Reference Material °C	Apparatus Constant A_c , W/m K
30	0.501
40	0.447
50	0.396
60	0.345
70	0.292
80	0.241
90	0.189
100	0.138

The thermal conductivity of concentrated whole milk was calculated employing equation 2 and its results are graphically presented in Fig. 2. This shows that the thermal conductivity increases with rise in temperature and decreases with increase in total solids content. This trend is in conformity with the literature (Konrad and Rambke 1971; Agrawala and Ojha 1972; Fernandez-Martin and Montes 1972). The effect of concentration on thermal conductivity is more prominent as compared to the effect of temperature. At 37% total solids content thermal conductivity increases from 0.455 W/m K at 40°C to 0.491 W/m K at 90°C

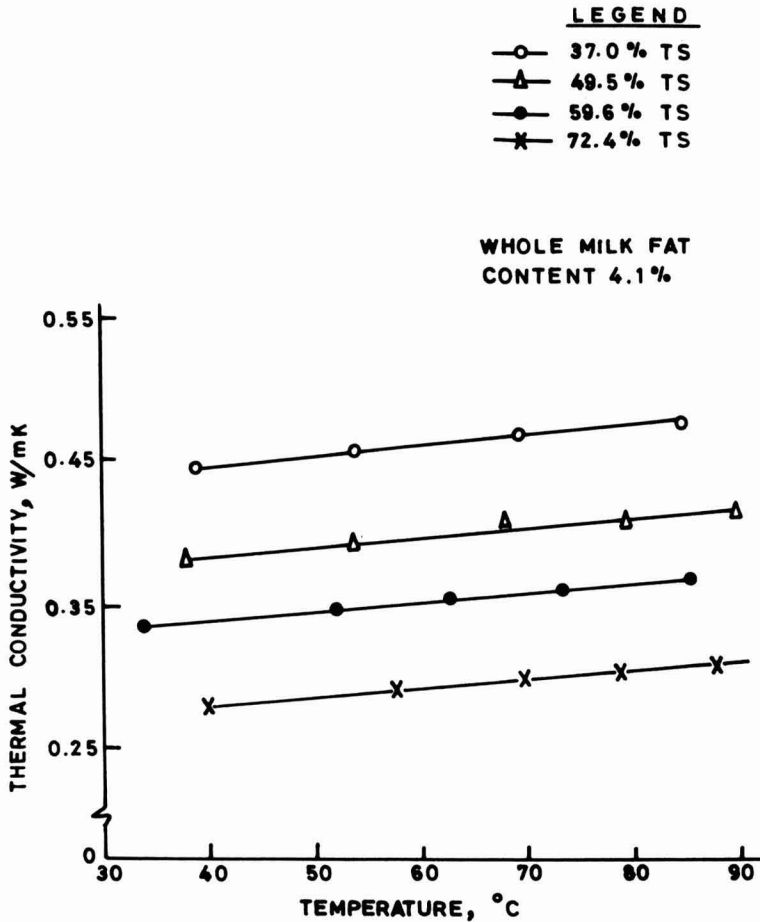


FIG. 2. VARIATION IN THERMAL CONDUCTIVITY OF WHOLE MILK WITH TEMPERATURE AT VARIOUS CONCENTRATIONS

(about 7.8% increase), whereas at 40° it varies from 0.455 to 0.278 W/m K (about 38.8% reduction) by increasing total solids content from 37 to 72.4%. This shows about 0.005 W/m K reduction in this thermal property with 1% increase in total solids compared to 0.00072 W/m K increase with 1°C rise in temperature. The temperature of each sample was calculated from the mean of top and bottom temperature during the test.

Following equation is developed from the experimental data of thermal conductivity of whole milk. The form of equation is based on the expression proposed by Riedel (1949).

$$K = (0.59 + 0.0012 T) (1 - 0.0078 X) \tag{4}$$

Where the thermal conductivity K of whole milk is related to its total solids percentage ($37 < x < 72$) and temperature ($40 < T < 90^\circ\text{C}$). Calculated values from the expression fits the respective experimental data within $\pm 0.88\%$.

NOMENCLATURE

- A Cross section of area, taken at right angle to the direction of heat flow, m^2 .
- A_c Apparatus constant and is equal to the ratio of K_p and x_p/x_m , W.m K .
- K Thermal conductivity, W.m K , K_d for distilled water, K_m for milk, K_p for perspex material.
- q Rate of heat transfer, W .
- T Temperature, $^\circ\text{C}$; T_1 and T_2 are the temperatures at the top and bottom of the reference material and T_3 is temperature of sample bottom layer.
- X Percentage of total solids constant.
- x Thickness in m , x_p for perspex and x_m for milk.

REFERENCES

- AGRAWALA, S. P. and OJHA, T. P. 1972. Effect of concentration on thermal conductivity of whole milk. *Indian J. Ag. Engg.* 9(3), 24-30.
- BATES, O. K. 1936. Thermal conductivity of liquid. *Ind. Engg. Chem.* 25(1), 4-31.
- DE, S. and RAY, S. C. 1952. Studies on indigenous method of khoa making. Part I. *Indian J. Dairy Sci.* 5(3), 147-165.
- FERNANDEZ-MARTIN, F. and MONTES, F. 1972. Influence of temperature and composition on some physical properties of milk and milk concentrates. III. Thermal conductivity. *Milchwissenschaft*, 27(12), 772-776.
- KONRAD, H. and RAMBKE, R. 1971. Physical properties of fluid milk concentrates. *Nahrung* 15(3), 269-277.
- LEIDENFROST, W. 1959. Measurement of thermal conductivity of milk. *ASME Symp. on thermal properties*, 291-294.
- MOHSENIN, N. N. 1980. *Thermal Properties of Foods and Agricultural Materials*, Goden Beach Science Publishers, New York.
- RIEDEL, L. 1949. Measurements of thermal conductivity in sugar solutions, Fruit juices and milk. *Chem. Ing. Tech.* 21, 340.
- SAKIADIS, B. C. and COATES, J. 1955. Studies of thermal conductivity. *Trans. ASME* 719.
- SWEAT, V. E. and PARMELLE, C. E. 1978. Measurement of thermal conductivity of dairy products and margerines. *J. Food Process Eng.* 2(3), 187-197.

HEAT TRANSFER IN THIN-FILM WIPED-SURFACE EVAPORATION OF MODEL LIQUID FOODS

KRZYSZTOF STANKIEWICZ¹ and M. A. RAO

*Institute of Food Science
New York State Agricultural Experiment Station
Cornell University, Geneva, New York 14456*

Accepted for Publication November 12, 1987

ABSTRACT

Experimental product-side heat transfer coefficients were studied in a laboratory scale thin-film wiped-surface (TFWS) evaporator under different rotational speeds, liquid flow rates and temperatures of the heating medium. Experiments were conducted with water, and 10, 30, and 45% sugar solutions in order to simulate the conditions during evaporation of fruit juices. Dimensionless correlations for heat transfer coefficient were established. It was shown that the "equivalent diameter" of the liquid bow wave formed in the front of wiper blade could be used as a characteristic dimension. Magnitudes of unstable and stable modes of evaporator performance were determined and different regimes related to the liquid flow were revealed.

INTRODUCTION

Thin-film mechanical evaporators are extensively used in food and chemical industries for concentration of high viscosity or heat sensitive products. The major advantages of such units are associated with the mechanical action of rotating close-clearance blades which considerably improve product-side heat transfer coefficients. Vigorously agitated liquid films are continuously removed from the heat transfer wall by the blades and due to very short contact times product degradation is minimized.

¹Present address: Department of Fruit and Vegetable Processing, Institute of Fermentation Industry, Warsaw, Poland.

²Address correspondence to author Rao.

Although thin-film mechanical evaporators have been known for a long time, very little information explaining heat transfer phenomena in these units can be found in published literature. Few theories that explain heat transfer phenomena in mechanically agitated liquid films can be found in review articles such as that of Harrod (1987) and Abichandani *et al.* (1987a). In contrast theories have been developed for liquid-full scraped-surface heat exchangers (without phase change) however, their usefulness for thin-film mechanical evaporation has not been proved.

Data on thin-film mechanical evaporators are also scarce because of very complex flow patterns and heat transfer phenomena in such systems. The majority of research work in the past was directed towards the influence of process parameters on the performance of thin-film evaporators, rather than on explanation of heat transfer and hydrodynamic phenomena in them. In general, it is recognized that many physical forces that influence liquid films create different regimes of evaporator operation. However, extremely limited and sometimes contradictory information is published on the specific ranges of evaporator operation and the effects of process variables on their magnitudes.

This study on heat transfer in TFWS evaporation was undertaken with the following objectives: (1) modeling the heat transfer in an TFWS evaporator and establishing dimensionless correlation under the wide range of variables studied, (2) to determine the effect of process variables on the wiped-film heat transfer coefficients, and (3) to recognize the modes of evaporator operation and determine the range of the specific regimes.

Fruit juices are sensitive materials and they can degrade when subjected to high temperatures. Therefore, we simulated conditions during commercial vacuum concentration of fruit juices. As model liquids water and sugar solutions were employed, because their physical properties are similar to those of fruit juices.

REVIEW ON MODELLING OF HEAT TRANSFER

Heat transfer in mechanical thin-film evaporators is affected by flow pattern as well as by boiling mechanisms. Liquid film thickness varies in such units both axially and circumferentially. According to visual observations (Bott and Romero 1966; Kiss *et al.* 1977; Nakamura and Watanabe 1982), the rotating wiper pushes the liquid layer in front of it forming so called "bow wave" or "liquid fillet". The thickness of a liquid film flowing vertically down decreases due to reduction in volume as a result of evaporation. Under certain process conditions, when fluid flow rate is lower than a specific minimum value, the heat transfer wall can become partially nonwetted, and so called "hot spots" are formed on the surface.

The complexity of the flow pattern is enhanced due to the boiling phenomena. A number of researchers (Lustenader *et al.* 1959; Bott and Romero 1966) main-

tained that the evaporation process takes place only from the interface between the liquid film and the vapors, and that the violent wiping action at the heat transfer surface suppresses nucleation. However, contrary opinion was presented by Ziolkowski and Skoczylas (1966). They assumed that there is nucleate boiling inside the product film, and that the presence of vapor bubbles enhances turbulent flow conditions and controls the intensity of heat transfer. According to Frank and Lutcha (1980) both boiling mechanisms could be expected in thin-film mechanical evaporation and the hydrodynamic conditions of the boiling film are related to the specific heat fluxes. At low values of heat flux and under laminar flow, evaporation takes place mainly from the surface. This mechanism is altered after attainment of a critical value of the heat flux and then heat transfer takes place due to vapor bubbles formed at the heat transfer surface or at overheated spots inside the film. Visual observations confirmed that both boiling mechanisms existed during evaporation from falling liquid films.

Bott and Sheikh (1964) suggested that the flow pattern and heat transfer in thin-film evaporators depends on the blade system design and its characteristics. Differences in flow patterns and the influence of process variables on it were also claimed especially between hydrodynamic blades (with self-aligning minimum clearance between the blade tip and the wall) and fixed-blades (blades rigidly fastened to the shaft to five constant clearance, usually 1-3 mm) (Skoczylas 1967).

Because of very complex flow patterns, mathematical analyses of heat transfer in thin-film wiped-surface evaporation are based usually on simplified models.

Dimensionless Correlations

A number of articles have been published in which attempts were made to establish correlations for heat transfer coefficient during TFWS evaporation. Different dimensionless groups have been employed that represent physical forces expected to be significant.

Selection of the characteristic dimension groups seems to be very difficult. Bott and Sheikh (1966) attempted to use an evaporator internal tube diameter as a characteristic dimension in wiped-surface evaporation of water-glycerol solutions (45, 62, and 85%). They assumed no nucleate boiling in the conditions of their experiments and established the correlation:

$$\text{Nu} = \text{Re}^{0.25} (\text{Re}_r)^{0.43} \text{Pr}^{0.3} \text{B}^{0.33} \quad (1)$$

Using the tube diameter as the characteristic dimension probably gives only approximate results, because the real flow patterns of the thin films may be neglected.

In other models, the thickness of liquid film was employed as the characteristic dimension. This approach, however, has disadvantages because calculation of the average film thickness of the evaporating film is very difficult. Several authors

presented equations for calculation of film thicknesses (Taeymans 1983; Abichandani *et al.* 1987b), but their usefulness is usually limited. Frank and Lutcha (1980, 1981) presented an equation for calculation of heat transfer coefficients for water and sugar solutions in a fixed-blade thin-film evaporator using film thickness as a characteristic dimension:

$$Nu_m = 2.5 \cdot 10^{-3} Re^{0.357} We_m^{0.183} (1 + 0.566 \cdot Pr^{0.35} K_1^{1.13}) \quad (2)$$

where the film thickness was calculated from the equation:

$$m = 0.368 \{(\eta/\rho)^2/g\}^{1/3} Re^{0.368} (\Pi_1)^{0.0052} (w_{av}/u)^{0.094} \quad (3)$$

Ziolkowski and Skoczylas (1966) assumed that the heat transfer is influenced by turbulent flow of the evaporating liquid layer, which is controlled by the size of vapor bubbles formed on the heat transfer surface. According to the heat transfer theory, bubble diameter equals $(\sigma/\rho g)^{0.5}$. The product-side heat transfer coefficient was assumed to be independent of the temperature difference across evaporating film and the liquid feed rate when the surface was completely wetted. They presented the correlation:

$$(Nu)^* = 3103.53 [(Re_r)^*]^{0.4039} Pr^{-1.053} K_2^{-0.3264} (\Pi_2)^{-0.494} \quad (4)$$

The same authors also presented an alternative expression, where internal tube diameter D was used as the characteristic dimension:

$$Nu = 839.151 (Re_r)^{0.3975} Pr^{-0.92} K_2^{-0.2361} Ga^{0.5995} (\Pi_3)^{-1.019} \quad (5)$$

As has been mentioned before, visual observations proved that the "bow wave" exists as an important element of flow pattern in mechanically agitated thin films. Mathematical analyses of the geometry of "bow wave" have been made by Kern and Karakas (1959) and Bott and Romero (1966). Their simplified models for TFWS evaporation contained the geometry of the "bow wave" as a characteristic dimension. This dimension, called "equivalent diameter", was calculated as:

$$D_e = 5.492 \cdot (M \eta / \rho^2 g B)^{0.25} \quad (6)$$

The above definition of the "equivalent diameter" was applied by other researchers also. Bott and Romero (1966) and Bott and Azooory (1969) used this parameter for establishing the correlations for heat transfer (without evaporation) in thin-film scraped-surface heat exchangers. Jian and Yu (1984) developed the correlation for heat transfer in fixed-blade thin-film evaporation of water and CMC-water solutions (0.1655-1.489%); the later are non-Newtonian shear-thinning liquids. Experimental data for CMC-water solutions were correlated by the dimensionless equation:

$$Nu_e = 1.3503 (Re)_e^{0.393} (Re_r)_e^{0.22} Pr^{0.4} (L/D_e)^{-0.4} \quad (7)$$

and data for water by:

$$Nu_e = 0.21942 \cdot 10^{-3} (Re)_e^{0.724} (Re_r)_e^{0.534} Pr^{0.4} (L/D_e)^{-0.4} \quad (8)$$

Correlations presented above were established for specific ranges of process variables studied but generally no information is given on different regimes of evaporator operation. In the study on heat transfer in a thin-film scraped-surface heat exchanger without phase change, Bott and Azoory (1969) reported two different flow regimes of fluid flow controlled by flow Reynolds number: "laminar" for $Re = 100$ and "transition" for $Re = 100 - 1000$.

MATERIALS AND METHODS

Experimental data were obtained during nearly 350 runs conducted with model liquid foods: water and 10, 30, and 45% sugar solutions. Magnitudes of studied process parameters are listed in Table 1.

TABLE 1.
PROCESS PARAMETERS

evaporation temperature, °C	50
steam temperature, °C	110, 130
rotational speed, rpm	70, 150, 500, 900, 1300
liquid feed rate, kg/hr	23, 58, 87, 132
evaporated solutions	water and water-sugar solutions (10%, 30%, 45% sugar)

A schematic of the experimental installation is shown in Fig. 1. Liquid was pumped from a feed tank to the shell-and-tube heat exchanger, where it was preheated with steam to boiling temperature. The feed temperature was maintained within $\pm 1.5^\circ$ by means of a temperature controller. The feed solution entering the evaporator was spread with a rotating dial distributor mounted on the shaft, providing complete circumferential coverage of the surface by the liquid. Evaporation process took place under vacuum in the TFWS vertical evaporator, described in detail below. Evaporated vapors were separated from the concentrate in the glass separation chamber and condensed in two tubular water coolers placed in series. Condensate was pumped out and collected for measurements. Concen-

trated liquid was pumped out with a Waukesha pump to a collecting tank. After volumetric measurements, condensate and concentrate were remixed and the solution, after a check of the sugar content, was returned to the feed tank.

Evaporator

A vertical TFWS evaporator made up of a "304" type stainless steel pipe 51.6 mm inside diameter, 213.0 mm long, with a wall thickness of 4.0 mm, equipped with a steam jacket, was constructed in the Department of Food Science and Technology, NYS Agricultural Experiment Station. The heat transfer area was 0.0371 m². The evaporator was equipped with three floating carbon wiper blades carried on the shaft. The blades were slotted on the surface. Three thermocouple wells were incorporated for the measurement of heat transfer wall temperature.

According to different names given to the blade systems in the literature, the blades used by us could be called "hydrodynamic blades", or "zero clearance carbon wipers" (Freese and Glover 1979), or "Smith blades" (Nakamura and Watanabe 1982).

Measurements

For wall temperature measurements thermocouples made from 0.25 mm Teflon coated copper-Constantan wires were employed. They were placed inside heat resistant 5.0 mm diameter ceramic tubes that were inserted tightly into wells made in the heat transfer wall. Thermocouples placed in the evaporator wall were fastened with an epoxy cement. Prior to starting the experiments, all thermocouples were calibrated in a constant temperature bath at boiling and freezing points, and at other intermediated points against a standard mercury thermometer.

Experimental data were collected about 15 min. after temperatures and the other variables had stabilized. During the experiments all the measured parameters were controlled: feed, steam, and evaporation temperatures, absolute pressure in separator, feed rate, and rotational speed of wiper blades. All needed corrections were made immediately. Runs were interrupted and repeated if detected differences between assumed and measured values were higher than $\pm 2\%$. All runs were duplicated.

All temperatures were recorded on an Apple II+ microcomputer with the aid of a data logger (Digistrip III, Kaye Insts.). Temperatures were recorded onto discs every 10 s.

Rotational speed of the shaft with wipers was measured with a tachometer. Absolute pressure inside separator was measured with a set of mercury manometers. Feed rate was calculated from the electronic scale readings of the weight of the feed tank. Condensate and concentrate rates were calculated from the weighted amounts of liquids collected during the run. Steam pressure in the jacket (dial manometer) and vacuum level after the condenser (dial vacuumeter) were noted. Sugar content in feed solution and concentrate were determined with a refractometer.

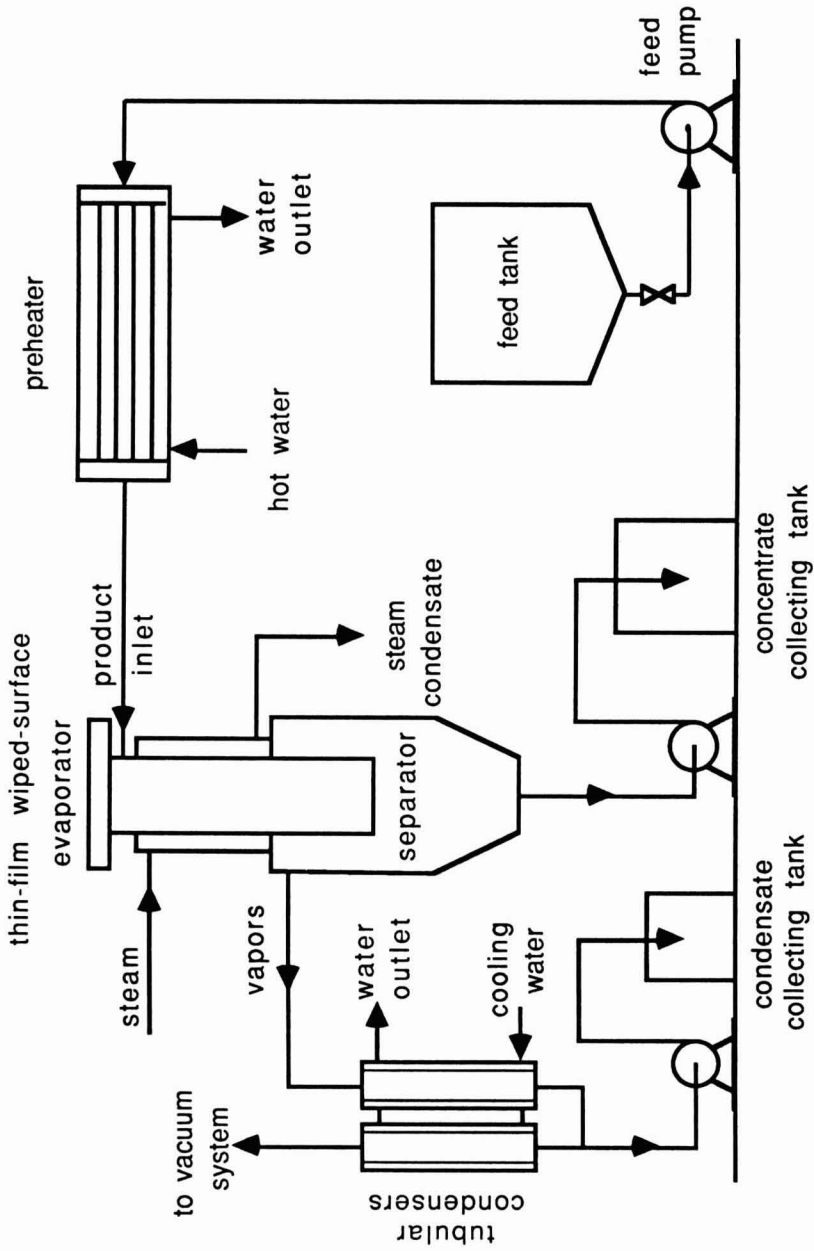


FIG. 1. SIMPLIFIED FLOW DIAGRAM OF EXPERIMENTAL INSTALLATION

Calculations

Magnitudes of the heat transfer coefficients were calculated using a program written in Fortran language and dimensionless correlations were established using a statistical program (Minitab, Pennsylvania State Univ.) on a Prime 9750 computer.

Wiped-Film Heat Transfer Coefficient

The amount of heat transferred to process liquid from the condensing steam consisted of sensible and latent heat. Latent heat was calculated from the amount of collected condensate. Generally, the feed temperature was very close to evaporation temperature (within $\pm 3.0^\circ\text{C}$), so that the effect of sensible heat could have been neglected. Nevertheless, sensible heat calculations were included in the computer program to make the results as precise as possible.

Magnitude of latent heat was calculated from the equation:

$$Q_L = M_C r \quad (9)$$

Sensible heat was calculated from the equation:

$$Q_S = M_f C_p (t_b - t_f) \quad (10)$$

If $t_f < t_b$ liquid had to be preheated inside evaporator to boiling temperature. Consequently, total heat flux was calculated as:

$$Q = Q_L + Q_S \quad (11)$$

Linear variation was assumed between adjacent measuring points and an average wall temperature was calculated as a mean weighted temperature:

$$t_w = (t_1 + 2 \cdot t_2 + t_3) / 4 \quad (12)$$

The overall heat transfer coefficient included wiped-film heat transfer coefficient and wall coefficient was calculated from the equation:

$$U = Q / [A(t_w - t_b)] \quad (13)$$

The product heat transfer coefficient was then obtained from the equation:

$$h_p = 1 / (1/U - \delta / \lambda_w) \quad (14)$$

where δ is wall thickness between the thermocouples and the inner tube surface. In our evaporator $\delta = 1.5$ mm. Thermal conductivity of "304" type stainless

steel was taken from literature (Kreith 1958) and for computer calculations linear relationship between λ_w and wall temperature was established from tabulated data as:

$$\lambda_w = 0.0243 t_u + 13.84 \quad (15)$$

where t_u is mean wall temperature between thermocouples and the inside wall surface.

Physical properties of water and sugar solutions were taken from literature and then mathematical expressions for them were derived for calculating the dimensionless groups.

Physical properties of evaporated solutions (besides η_w) were calculated at the measured boiling temperature. The physical properties of sugar solutions were determined for average sugar content during the evaporation, i.e., between the feed solution and the concentrate. Average axial mass flow rate was calculated as the arithmetic mean value of the feed and concentrate rates.

RESULTS AND DISCUSSION

Modes of Evaporator Performance

Based on the computer records of the wall temperatures as a function of time and the range of variables studied the performance of the evaporator can be divided into stable and unstable modes. Unstable range was found for lower wiper rpm values and feed rates. Generally, unstable mode of operation was characterized by unexpected and large fluctuations in the measured wall temperatures as a function of time. Fluctuations recorded during evaporation of water are presented in Fig. 2. Within unstable range, significant temperature changes were noticed during short periods of time. After increasing the rotational speed or the feed rate above the specific values, such fluctuations completely disappeared and the wall temperatures remained almost constant.

It was also found that for unstable mode of operation wiped-film heat transfer coefficients were considerably lower compared to those for the stable mode. It is likely that, under specific process conditions, within the unstable mode of evaporator performance part of heat transfer surface was not wetted by the liquid, so that partly dry overheated regions were formed on the wall and these in turn produced the measured strong fluctuations in evaporator wall temperature. Detailed analysis of the physical phenomena responsible for unstable conditions during evaporation is presented below.

Experimental data obtained within unstable mode of operation have not been applied for establishing correlations and the analysis presented below deals only with the stable mode.

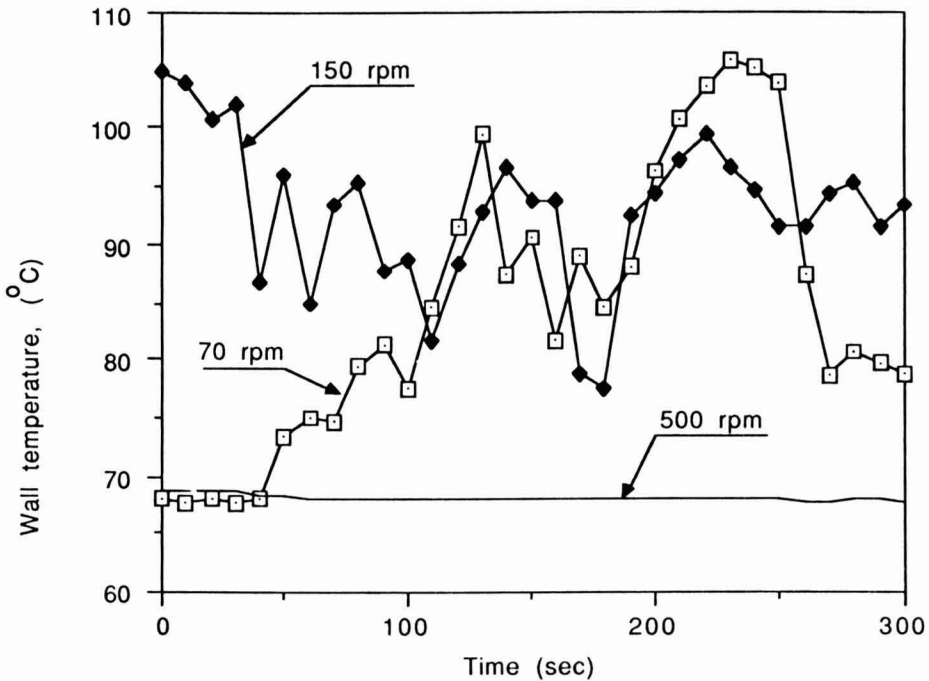


FIG. 2. FLUCTUATIONS OF MEASURED WALL TEMPERATURES DURING THIN-FILM WIPED-SURFACE EVAPORATION OF WATER

Regimes of Fluid Flow

Influence of the rotation speed N on the heat transfer coefficient presented in Fig. 3 for 23 kg/h and $t_s = 130^\circ\text{C}$ can be divided into three regions. For $N = 70$ -150 rpm relatively low values of h_p were noticed for all liquids and these were related to unstable mode of operation. Further increasing N resulted in increase of h_p but after attainment of 500 rpm h_p became almost constant for N values up to 1300. Additional measurements conducted with water within the rpm range of 150-500 rpm revealed that for 70-200 rpm the evaporator operation was unstable. In the rpm range of 250-350, rapid increase in heat transfer coefficient was noticed within stable mode of operation.

The two different regions found for stable mode could be called "transition" and "turbulent" regimes. Magnitudes of process parameters for both regimes are presented in Fig. 4. Laminar regime could exist within the mentioned unstable mode of operation. However, there is no evidence that the above names represent flow regimes similar to those known from fluid mechanics theory. The different physical behavior noticed in the regions was related to specific liquid flow velocities (both axial and circumferential) but probably also were influenced by the boiling mechanism or the other physical forces that existed in the system.

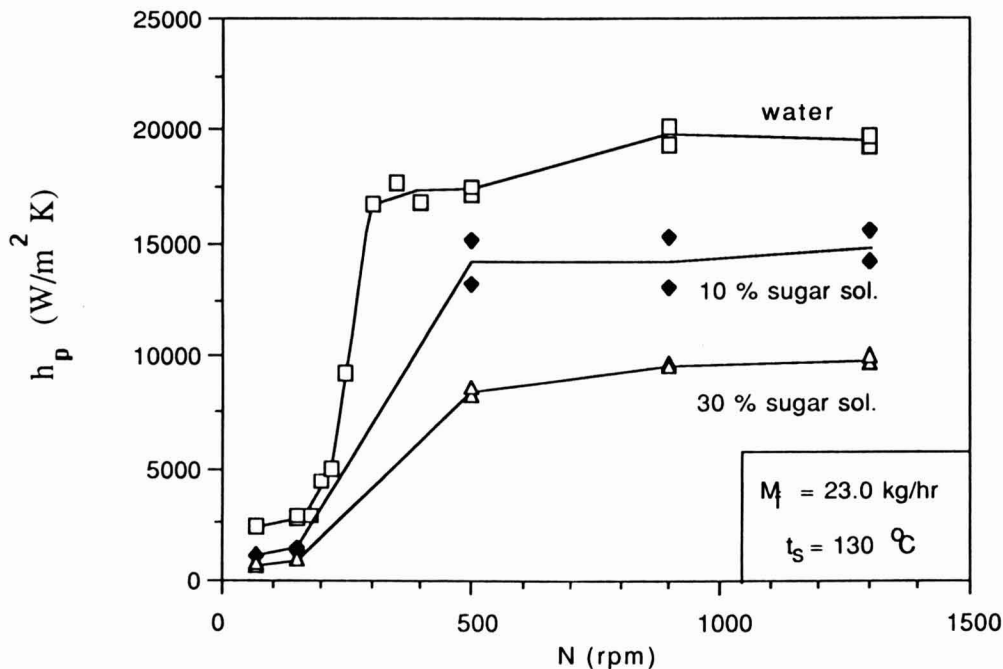


FIG. 3. EFFECT OF ROTATIONAL SPEED ON HEAT TRANSFER COEFFICIENT

Correlations for Heat Transfer

Separate dimensionless correlations for heat transfer in transition and turbulent regimes were established. Unstable mode was omitted from the analysis.

For the modeling of heat transfer in TFWS evaporator we selected Nusselt (Nu_e), Prandtl, Reynolds (Re_e), and Froude (Fr_e) numbers. These dimensionless groups were derived from theoretical analysis by Bott and Azoozy (1969) and they represent physical phenomena expected during TFWS evaporation. Froude number was included instead of rotational Reynolds number because it represents the ratio between centrifugal and gravitational forces in thin-film mechanical evaporators. We assumed that evaporation in the descending fluid took place mainly in the "bow wave", so that the characteristic dimension used was the equivalent diameter D_e of a triangular liquid fillet as defined by Bott and Romero (1966).

The temperature difference across the wiped film was assumed to influence heat transfer coefficient and it was taken into consideration by the factor (η/η_w) , which is the ratio between product viscosities in boiling liquid and wall temperature, respectively. Finally, the general correlation for TFWS evaporation was assumed to be:

$$Nu_e = a (Re_e)^b Pr^c (Fr_e)^d (\eta/\eta_w)^e \quad (16)$$

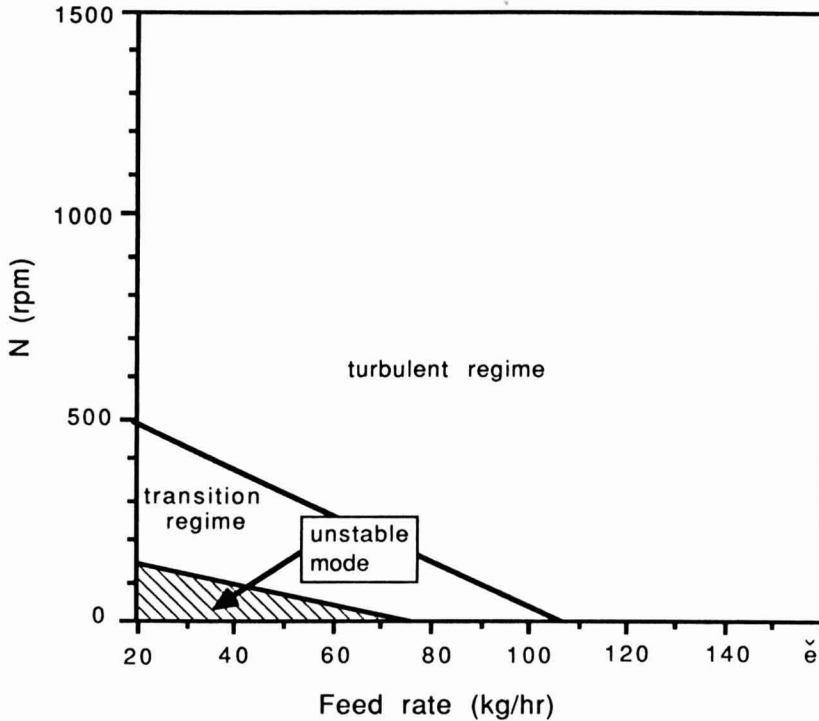


FIG. 4 RANGES OF MODES AND REGIMES OF EVAPORATOR PERFORMANCE

where a , b , c , d and e are constants to be determined. Constant “ a ” depends on the geometry of an evaporator as well as number and arrangement of blades.

The correlation obtained for the transition regime was:

$$Nu = 0.0483 Re^{0.586} Pr^{1.05} Fr^{0.118} (\eta/\eta_w)^{-2.93} \quad (17)$$

Equation (17) is valid for: $M_f = 58-87$ kg/h and $N = 150-500$ rpm.

The correlation obtained for the turbulent regime was:

$$Nu = 4.137 Re^{0.263} Pr^{0.325} Fr^{0.032} (\eta/\eta_w)^{-0.753} \quad (18)$$

Equation (18) is valid for: $M_f = 87-133$ kg/h and $N = 500-1300$ rpm. The magnitudes of R^2 for Eq. (17) and (18) were 0.96 and 0.63, respectively.

Effect of Process Variables on Heat Transfer Coefficient

Calculated product-side heat transfer coefficient obtained within wide range of process variables allowed us to analyze the influence of studied parameters on the evaporator performance.

Figure 3 presents the magnitudes of heat transfer coefficients obtained during evaporation of different liquids. In general, the coefficients calculated under similar process conditions were higher for less viscous liquids, indicating the important role of viscosity in TFWS evaporation. It was also found, that the rules governing the influences of process variables on heat transfer coefficients were similar for all working liquids employed in our study.

Figure 5 shows the influence of rotational speed on the heat transfer coefficients for 10% sugar solutions. Only for the lower feed rates (23.0 and 58.0 kg/h) unstable mode and transition regime were detected. For $M \geq 87.0$ kg/h and $N \geq 500$ rpm heat transfer coefficients remained almost independent of both food rate and rotational speed.

In Fig. 6 and 7 variations of heat transfer coefficients with liquid feed rate are presented. h_p was influenced by the feed rate at low rotational speeds (70 and 150 rpm). Therefore, it appears that the axial flow rate controls the magnitude of flow regimes. For rotational speeds higher than 500 rpm almost no effect of feed rate on heat transfer was noticed.

The influence of two steam temperatures on heat transfer coefficient is presented in Fig. 8. Higher h_p values obtained within unstable mode of operation for lower steam temperature were probably due to the difference in specific heat flux. Considerably lower heat flux found for $t_s = 110^\circ\text{C}$ could be related to the gentle

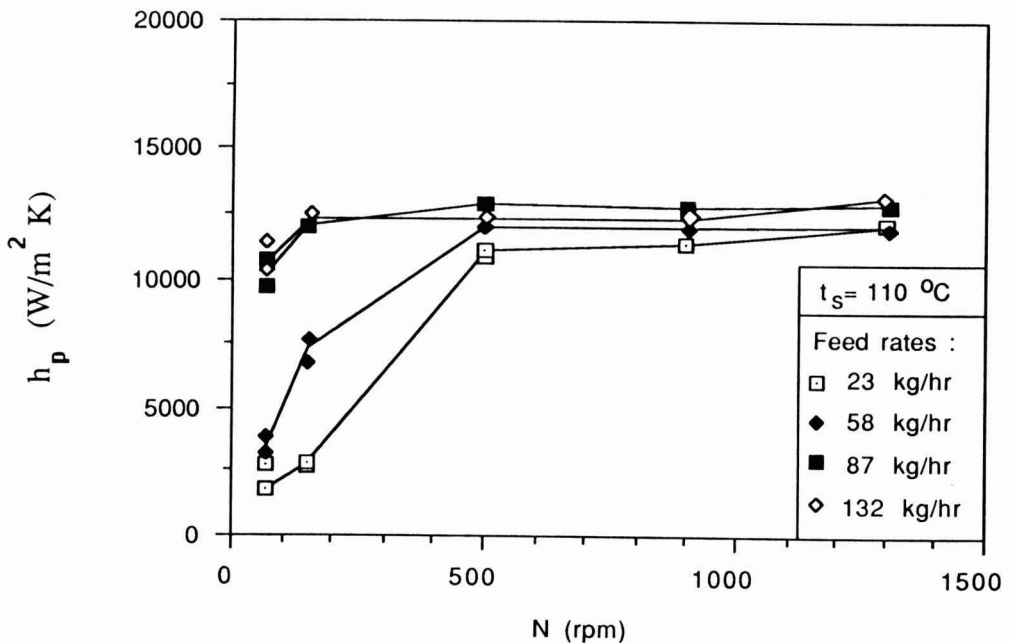


FIG. 5. EFFECT OF ROTATIONAL SPEED ON HEAT TRANSFER COEFFICIENT FOR 10% SUGAR SOLUTION

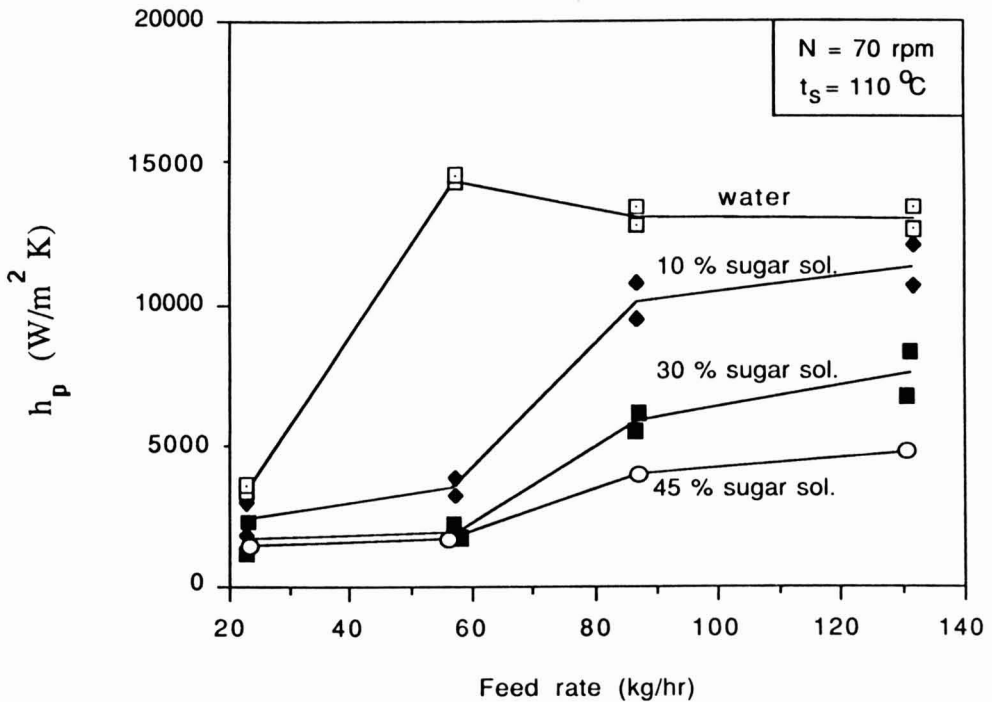


FIG. 6. EFFECT OF FEED RATE ON HEAT TRANSFER COEFFICIENT, $N = 70$

evaporation from the surface. It is likely that for $t_s = 130^\circ\text{C}$ nucleate boiling took place, which is associated with the formation of vapor bubbles on the heat transfer surface. Violent formation of overheated vapor bubbles could cause unstable conditions on the heat transfer surface. When the liquid film is very thin it can be easily disrupted by the vapor bubbles, thus partly unwetted regions are frequently formed on the wall. Such phenomenon, however, causes decrease in the effective heat transfer surface and consequently in the magnitude of the heat transfer coefficient. Increasing the rotational speed provides more uniform covering of the surface with the liquids and suppresses the formation of the unwetted regions. Similar effect is expected with increasing feed rate.

CONCLUSIONS

The experimental thin film evaporator was satisfactory for studying heat transfer rates. Thermocouples in the walls were useful for determining product side heat transfer coefficients and also for detecting unstable operation of the evaporator as indicated by large fluctuation in the measured wall temperatures. Unstable

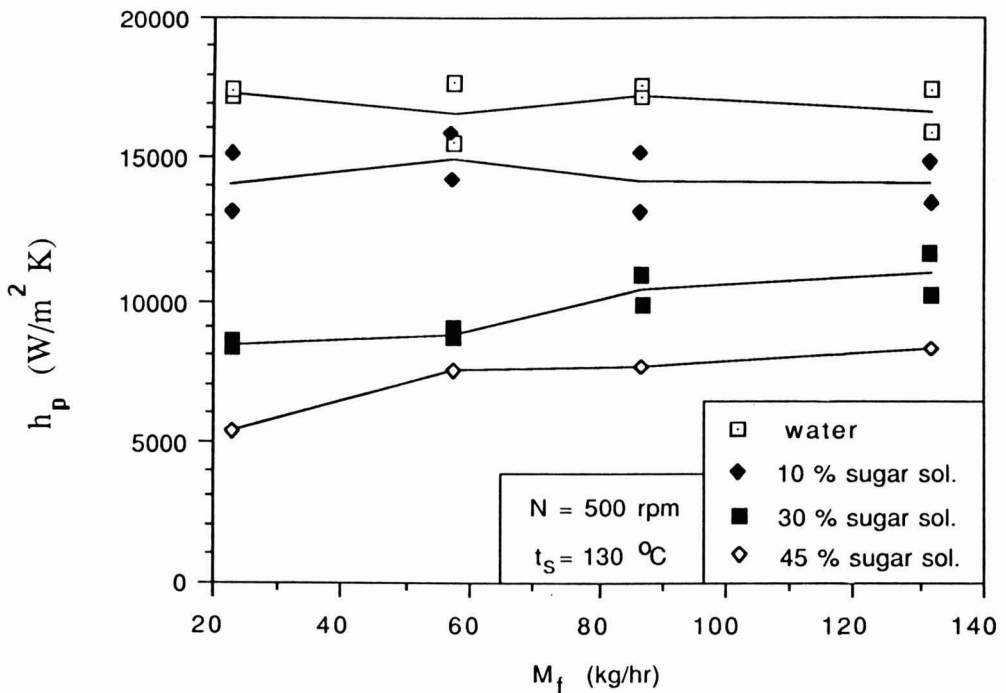


FIG. 7. EFFECT OF FEED RATE ON HEAT TRANSFER COEFFICIENT, N = 500

operation of the evaporator occurred when the rpm of the wiper blades was 70-150. Rapid increase in h_p was observed for rpm range 250-350. Under similar conditions of evaporation, magnitudes of heat transfer coefficient were lower for high viscosity liquids.

NOMENCLATURE

- a,b,c,d,e constants (Eq. 16)
- A heat transfer area, m²
- B number of blades on the shaft
- C_p product heat capacity, J kg⁻¹ K⁻¹
- D evaporator tube inside diameter, m
- D_e equivalent diameter (Eq. 6), m
- g acceleration due to gravity, m s⁻²
- h_p product-side heat transfer coefficient, W m⁻² K⁻¹
- m liquid film thickness, m
- M mean liquid mass flow rate during evaporation, kg s⁻¹

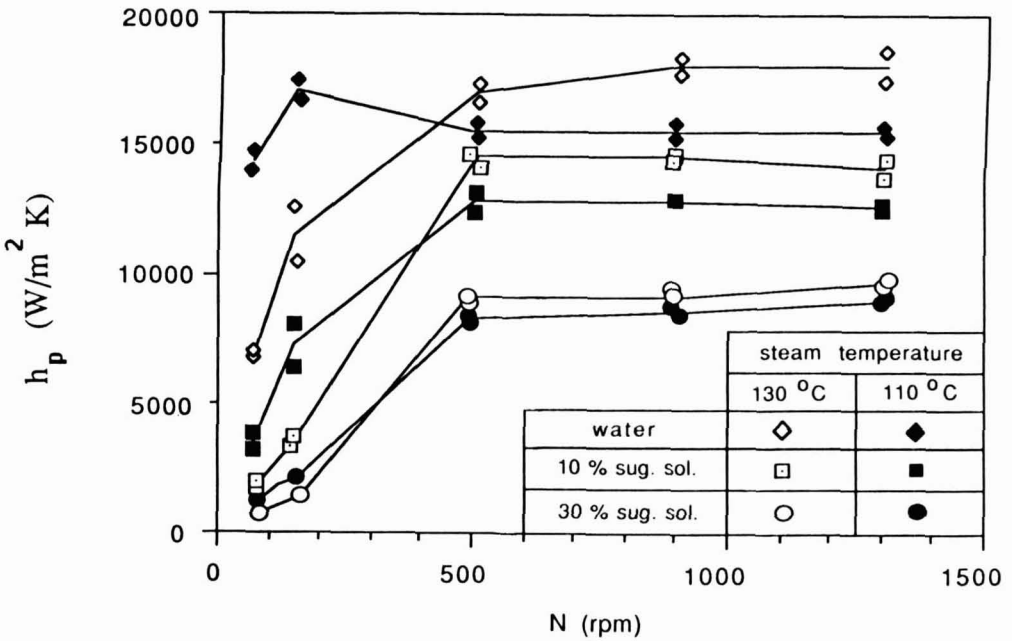


FIG. 8. EFFECT OF STEAM TEMPERATURE ON HEAT TRANSFER COEFFICIENTS, FOOD RATE 58 KG/HR

M_c	condensate flow rate, kg s^{-1}
M_f	mass flow rate of the feed solution, kg s^{-1}
N	rotational wiper speed, s^{-1}
q	heat flux, W m^{-2}
Q	total heat rate, W
Q_L	latent heat, W
Q_s	sensible heat, W
r	heat of evaporation of water, J kg^{-1}
t_b	boiling temperature, $^{\circ}\text{C}$
t_f	feed temperature, $^{\circ}\text{C}$
t_s	steam temperature, $^{\circ}\text{C}$
t_1, t_2, t_3	measured heat transfer wall temperatures, $^{\circ}\text{C}$
Δt_p	temperature drop across the liquid film, $^{\circ}\text{C}$
u	average axial velocity of film flow, ms^{-1}
U	heat transfer coefficient (Eq. 13), $\text{W m}^{-2} \text{K}^{-1}$
w_{av}	average circumferential velocity of film flow, ms^{-1}
x	sugar fraction in feed solution (kg/kg)

Greek letters

δ	heat transfer wall thickness between the thermocouple and inside diameter, m
λ	liquid thermal conductivity, $\text{W m}^{-1} \text{K}^{-1}$
λ_w	thermal conductivity of heat transfer wall, $\text{W m}^{-1} \text{K}^{-1}$
η	liquid viscosity, Pa.S
η_w	liquid viscosity in wall temperature, Pa.S
ρ	liquid density, kg m^{-3}
σ	liquid surface tension, N m^{-1}

Dimensionless groups

$Fr_e = N^2 D_e D / \eta$	Froude number for equivalent diameter
$Ga = g D^3 \rho^2 / \eta^2$	Galileo number (eq. 5)
$K_1 = r / C_p \Delta t_p$	criterion of the phase change (eq. 2)
$K_2 = r / C_p (t_b + 273.15)$	criterion of the phase change (eq. 4)
$Nu = h_p D / \lambda$	Nusselt number
$Nu_e = h_p D_e / \lambda$	Nusselt number (characteristic dimension - equivalent diameter)
$Nu_m = h_p m / \lambda$	Nusselt number (eq. 2)
$Nu^* = h_p (\sigma / \rho g)^{0.5} / \lambda$	Nusselt number (eq. 4)
$Pr = C_p \eta / \lambda$	Prandtl number
$Re = 4 M / \Pi D \eta$	Reynolds number
$Re_e = 8 M / D_e \eta B$	Reynolds number for equivalent diameter
$Re_r = N D^2 \rho / \eta$	rotational Reynolds number
$(Re_r)_e = N D D_e \rho / \eta$	rotational Reynolds number for equivalent diameter

$$(\text{Re}_r)^* = N D (\sigma/\rho g)^{0.5} \rho / \eta \quad \text{rotational Reynolds number (eq. 4)}$$

$$\text{We}_m = N^2 D^2 \rho m / \sigma \quad \text{Weber number (eq. 2)}$$

$$\Pi_1 = \rho \sigma^3 / g \mu^4 \quad \text{dimensionless group (eq. 3)}$$

$$\Pi_2 = (\sigma/\rho g)^{0.5} \sigma \rho / \eta^2 \quad \text{dimensionless group (eq. 4)}$$

$$\Pi_3 = \sigma \rho D / \eta^2 \quad \text{dimensionless group (eq. 5)}$$

ACKNOWLEDGMENTS

Author Stankiewicz gratefully acknowledges a Fulbright scholarship. The authors thank J. C. Moyer, Robert Miller, and Howard Casasanta for the design and fabrication of the evaporator, Bob Ennis for help and assistance during the experiments, and Herb Cooley for his contribution to computer programming.

REFERENCES

- ABICHANDANI, H., SARMA, S. C. and HELDMAN, D. R. 1987a. Hydrodynamics and heat transfer in liquid full scraped surface heat exchangers—A review. *J. Food Process Eng.* 9(2), 121-141.
- ABICHANDANI, H., SARMA, S. C. and HELDMAN, D. R. 1987b. Hydrodynamics and heat transfer in thin film scraped surface heat exchangers —A review. *J. Food Process Eng.* 9(2), 143-172.
- BOTT, T. R. and ROMERO, J. J. B. 1963. Heat transfer across a scraped surface. *Can. J. Chem. Eng.* 41, 213-219.
- BOTT, T. R. and SHEIKH, M. R. 1964. Effect of blade design in scraped surface heat transfer. *Brit. Chem. Eng.* 9(4), 229.
- BOTT, T. R. and ROMERO, J. J. B. 1966. The characteristic dimension in scraped surface heat transfer. *Can. J. Chem. Eng.* 44, 226-230.
- BOTT, T. R. and SHEIKH, M. R. 1966. Evaporation at a scraped surface. *Chem. Eng. Progr. Symp. Ser.* 62(64), 97-103.
- BOTT, T. R. and AZOORY, S. 1969. Heat transfer in scraped heat exchangers. *Chem. Proc. Eng.* 50(1), 85-90.
- FRANK, J. T. and LUTCHA, J. 1980. Thickness of the film of material treated in a film-type rotary evaporator. *Int. Chem. Eng.* 20(1), 65-76.
- FRANK, J. T. and LUTCHA, J. 1981. Heat transfer in a rotary film evaporator. *Chem. Prum.* 31(3), 109-114.

- FREEZE, H. L. and GLOVER, W. B. 1979. Mechanically agitated thin-film evaporators. *Chem. Eng. Prog.* 75, 52-58.
- HARROD, M. 1986. Scraped surface heat exchangers. A literature survey of flow patterns, mixing effects, residence time distribution, heat transfer and power requirements. *J. Food Process Eng.* 9(1), 1-62.
- JIAN, T. and YU, Y. 1984. Heat transfer characteristics of non-Newtonian liquid in wiped-film evaporator. *Huadong Huagong Xueyuan Xuebao* (3), 395-400.
- KERN, D. Q. and KARAKAS, H. J. 1959. Mechanically aided heat transfer. *Chem. Eng. Progr. Symp. Ser.* 55(29), 141-148.
- KISS, Z., FRESZ, I. and BUCKSKY, G. 1977. Determination of the shape and size of bow wave in rotary film equipment with wiping blades. Paper No. 4.08. Proceedings of the 3rd conference on Applied Chemistry Unit Operations and Processes. Veszprem, Hungary.
- KREITH, F. 1958. *Principles of Heat Transfer*. p. 533. International Textbook Co., Scranton, Pennsylvania.
- LUSTENADER, E. L., RICHTER, R. and NEUGEBAUER, F. J. 1959. The use of thin films for increasing evaporation and condensation rates in process equipment. *J. Heat Transfer* 81C, 297-307.
- NAKAMURA, K. and WATANABE, T. 1982. Flow in agitated thin film horizontal evaporator. *Chem. Eng. Commun.* 18, 173-190.
- SKOCZYLAS, A. 1967. Thin film evaporator construction and performance. *Brit. Chem. Eng.* 12(8), 1235-1239.
- TAEYMANS, D. 1983. Flow of newtonian fluids in mechanically agitated thin films. Paper presented at the International Symposium "Film techniques applied to chemical engineering operations". April 1983. Inst. Franc. Petrole, Rueil Malmaison, France.
- ZIOLKOWSKI, Z. and SKOCZYLAS, A. 1966. Heat transfer during thin-film evaporation of liquids in Sambah-type evaporator. *Chem. Stosowana* 2B, 227-271.

EXPERIMENTAL VERIFICATION AND USE OF PRESSURIZED CAN MODELS

PHILIP L. BREWBAKER¹

*Former Graduate Student in Food Science and Technology
University of California, Davis
National Food Processors
Berkeley, California 94710*

and

JERALD M. HENDERSON²

*Professor of Mechanical Engineering and
Food Science and Technology
University of California, Davis 95616*

Accepted for Publication March 4, 1988

ABSTRACT

The results of an experimental investigation of the strength characteristics of pressurized food cans are compared with existing models of thin-walled cylinders as they pertain to the common unbeaded can. After using the data to establish the empirical quantities in the models, good agreement was found between theory and experiment. The models were then used to predict strength characteristics of hypothetical cans.

INTRODUCTION

A recent experimental investigation of the strength characteristics of pressurized food cans was conducted to investigate potential material and thickness changes that might be possible if pressurization became a more popular processing option in the future (Brewbaker 1986).

¹Present address: Philip L. Brewbaker, National Food Processors Association, 1950 Sixth Street, Berkeley, CA 94710.

²Address correspondence to: Jerald M. Henderson, Mechanical Engineering, University of California, Davis, CA 95616, 916-752-1778.

Buckling of cylinders under external pressure has been studied extensively (Yamaki 1984). A useful semiempirical design approach that is relatively simple to use has been developed (Baker *et al.* 1972 CH. 10). This method estimates the panel resistance of a cylinder, after reducing its physical parameters to non-dimensional factors and provides a lower bound, which 90% of the cylinders should exceed. The method is applied to thin-walled cylinders and is accurate over a wide range of sizes and material strengths. This buckling model does not require the material yield point, only the dimensions and modulus of elasticity.

Buckling of cylinders in compression has been examined closely, and a useful design approach, which uses both theoretical and empirical factors, has been developed by Harris *et al.* (1957); and Baker *et al.* (1972; CH 10). This general method was developed from tests on a wide array of cylinder sizes and materials. The method predicts a buckling stress for unpressurized cylinders, then adds a factor to that stress if the cylinder is pressurized. As before, material yield points are not considered. From the Harris approach, the average load resistance is calculated, rather than a lower bound.

In the interest of brevity and because we used the referenced theoretical and empirical models without alteration this paper does not repeat any of the details, which can be obtained from the original references or the complete documentation (Brewbaker 1986) of this project.

The objective of this paper is to compare the results of this experimental study with existing thin-walled cylindrical models as they pertain to the common unbeaded can, and then use the verified models to predict the strength characteristics of some typical hypothetical cans.

MATERIALS AND METHODS

Two strength criteria were used in this study. One is the resistance to stacking loads, an axial load distributed around the top (and bottom) of the can. This *load resistance* is defined as the maximum distributed axial load, in pounds, that a can will withstand before significant deformation; a common compression testing device was used for this portion of the investigation. The other criterion is the resistance to side wall deformation due to external pressure. This *panel resistance* is defined as the maximum difference in external pressure and internal pressure in psig, totally surrounding the can that it will withstand before deformation; enclosed pressure vessels were used to obtain this data.

The steel three-piece, welded side seam cans used in this study were essentially common 303×406 food cans without beading. Thickness and temper were varied. Two common canmaking tinplate tempers were used. CAT4 tinplate is continuously annealed, while DR8 is double reduced. The DR8 temper is a stronger steel, used for making thin cans. The aluminum cans used in the tests were taken

directly from supermarket shelves and were unbeaded, twopiece cans with ends that were necked in and of the 206×406 size.

RESULTS AND DISCUSSION

Panel Resistance

All of the cans in this study failed by buckling when tested for panel resistance, and the experimental results showed no difference in the two steel tempers used.

Figure 1 shows the experimental results versus the predicted values. The model was capable of reproducing with fair accuracy the actual panel resistance of the cans. Differences between predicted and actual panel resistances was from 7% to 18% for the steel cans. The difference increased as thickness increased.

The difference between predicted and actual panel resistances may have been due to a faulty pressure gauge used in the experiment; many faulty Bourdon tube pressure gauges have an increasing discrepancy as the pressure increases. On the other hand, it may be due to the use of 90% lower bound predicted values. The method worked particularly well with the aluminum cans, despite their less than cylindrical shape.

Assuming the results to be accurate, the predicted values can be improved by multiplying by a constant of 1.1. The result is also shown in Fig. 1. The buckling method, designed originally for cylinders used in aircraft and rocketry, can be applied to the case of cans buckling under external pressure. It appears to be accurate as well for cans which are not quite cylindrical.

Load Resistance

In axial loading, the cans showed both yielding and buckling. These two failure phenomena are of course quite distinct, and so will be treated separately.

Figure 2 shows the load resistance results obtained in this study and associated predicted values for the cans which exhibited buckling, the DR8 steel cans and the aluminum cans, when unpressurized. CAT4 cans did not buckle in compression.

The buckling method was consistent in modeling the load resistance of the cans. Even the aluminum cans were fairly well approximated. The difference between predicted and actual values varied from 2% to 27%, with the predicted values always higher. This may be due to the fact that the buckling method theory was based on tests with carefully constructed cylinders. In buckling, any deviation from a perfectly cylindrical form can reduce the load resistance of a cylinder (Yamaki 1984). Therefore cans, because of their construction, may be further from a perfectly cylindrical surface than the test cylinders from which the buckling method was derived.

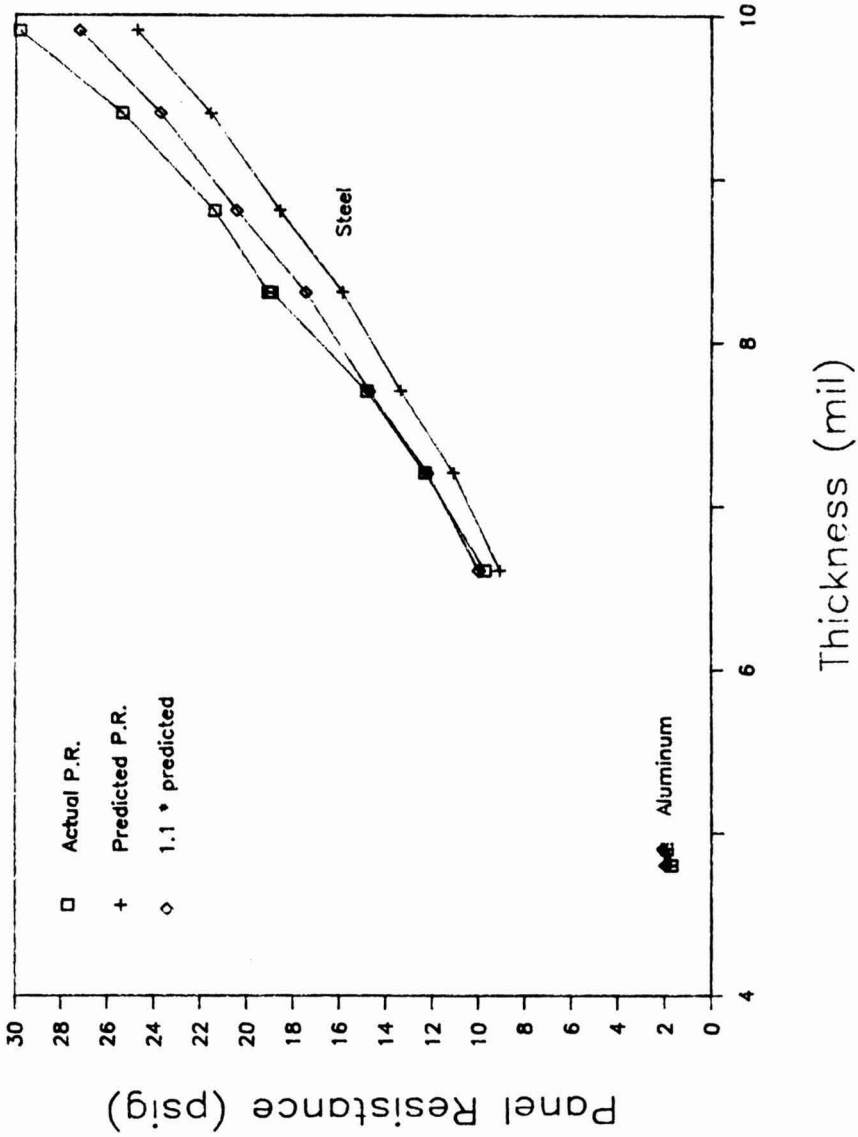


FIG. 1. PANEL RESISTANCE

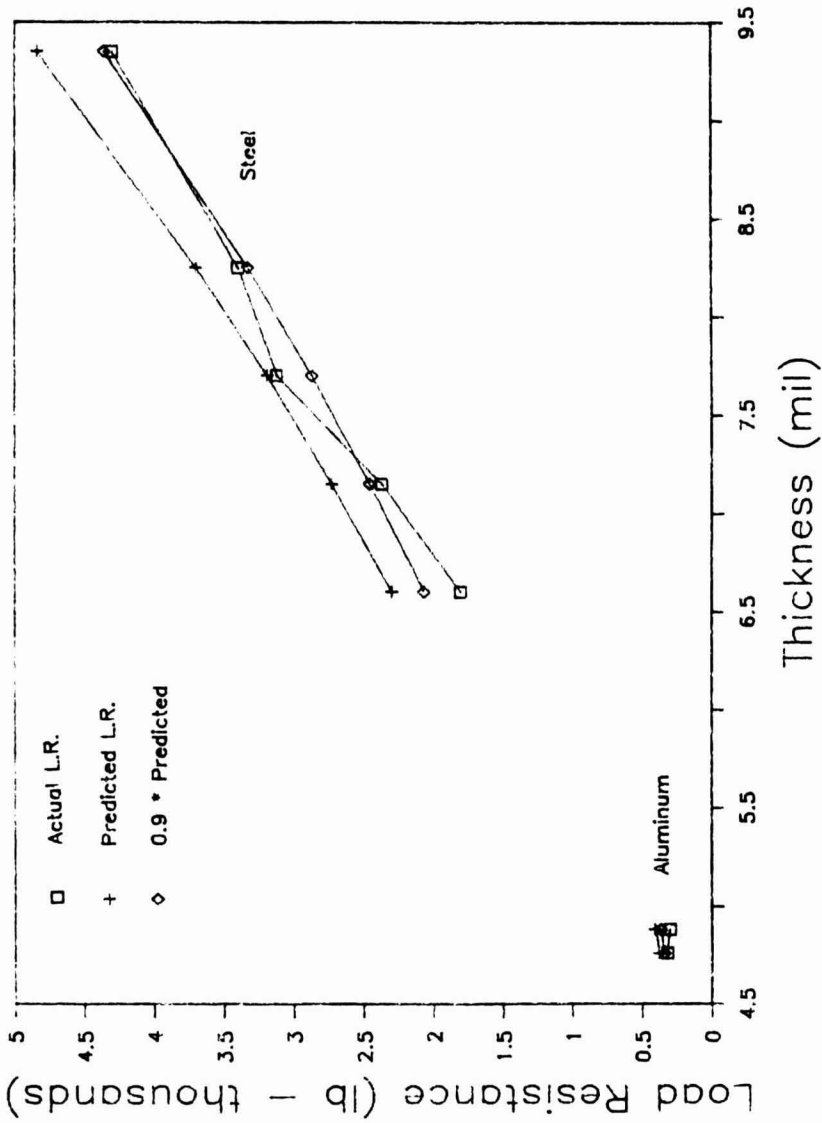


FIG. 2. LOAD RESISTANCE — for buckling failure

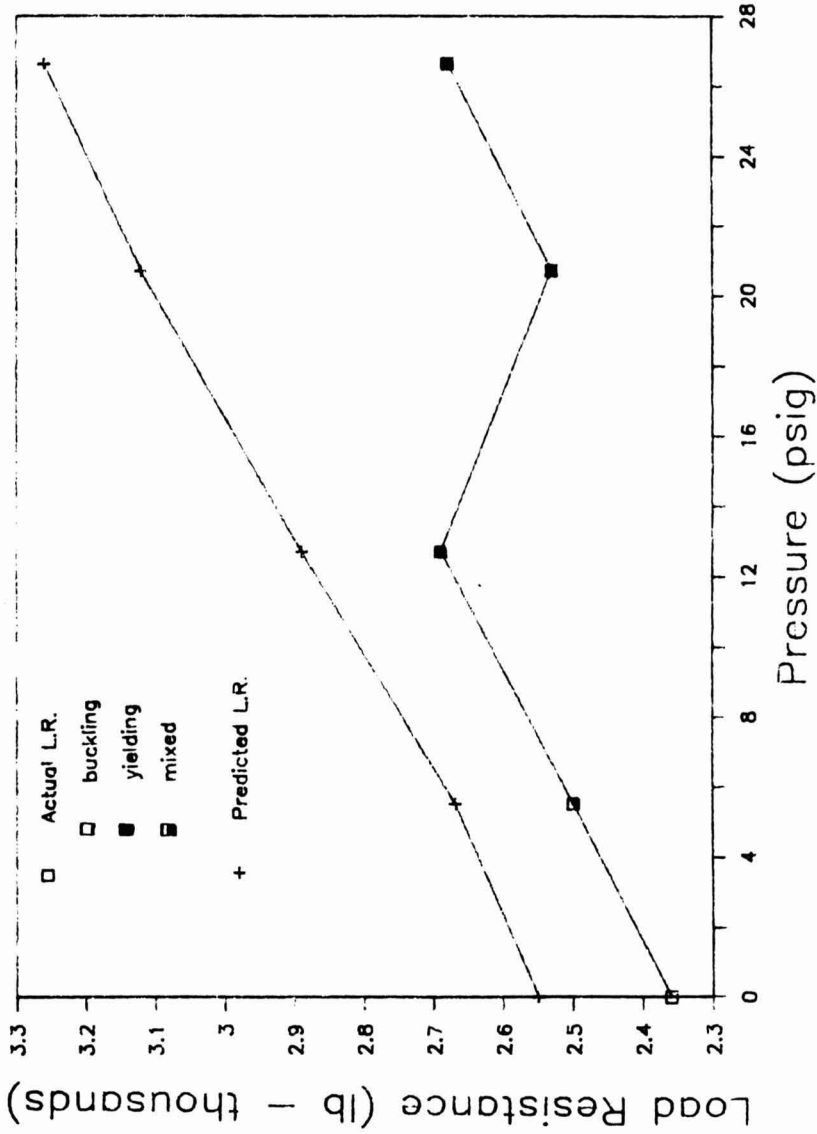


FIG. 3. LOAD RESISTANCE VS PRESSURE — for a 7.15 mil unbeaded steel can

By placing a factor, 0.9, before the predicted load resistance values, the agreement between predicted and actual results can be increased, Fig. 2.

The model used predicts that the load resistance of a can should increase as its internal pressure is increased. For example, Fig. 3 shows the predicted versus actual load resistance of a 7.15 mil steel can as a function of its internal pressure. Although the results follow the model at low pressure, at higher internal pressures yielding became the predominant failure mode.

Yielding of cans in compression occurs when the stress at any location in the can exceeds the yield strength of the material. Such yielding leads to failure of the can; other shapes may deform to a configuration of greater load bearing strength, but this is not true of cylinders. In compression, then, determining the load at which can failure thru yielding will occur is reduced to finding the point of maximum stress in the sidewall and calculating the load at which that stress will exceed the yield strength of the material.

Unfortunately, finding the stress at every point in the can is difficult without certain assumptions. Most importantly, the can must be assumed symmetric about its long axis. Also, the load must be applied symmetrically about that axis. With these assumptions, points on the sidewall that are on the same horizontal plane of the can will have identical stresses.

In this study, the different can types tested for load resistance yielded at different internal pressures. For example, the DR8 steel cans generally yielded at pressures above 12 psig. The aluminum cans yielded at 43 psig, the only pressure at which they were tested. The CAT4 steel cans yielded at all pressures, including zero pressure.

The simplest way to calculate stresses in a compressed can is to assume that it is a perfect cylinder loaded vertically at the edges and internally by pressure. Assuming there were no secondary edge loadings on the sidewall, stresses within the can would be due to the primary loads: compression and pressure. For a given internal pressure an iterative process is required to find the load resistance. The resistance values calculated by this method, are from 1.7 to 2.7 times higher than the actual results.

This method assumes the absence of edge loads. However, edge loads must have been present, because in every case, yielding occurred at the edge of the sidewall, near the lid.

A simple edge load which must have been present in these cans was the moment created by eccentric loading. Because of the way the cans are lidded, the compressive load was actually loading the can along a circle of slightly greater radius than that of the sidewall, Fig. 4. The difference is labelled Δ . For the purposes of modeling this load, the eccentric load, can be replaced with an equivalent load and a moment. The moment would be along the edge, bending it outward. If Δ is not too large, the magnitude of the moment would be equal to the compressive load times Δ .

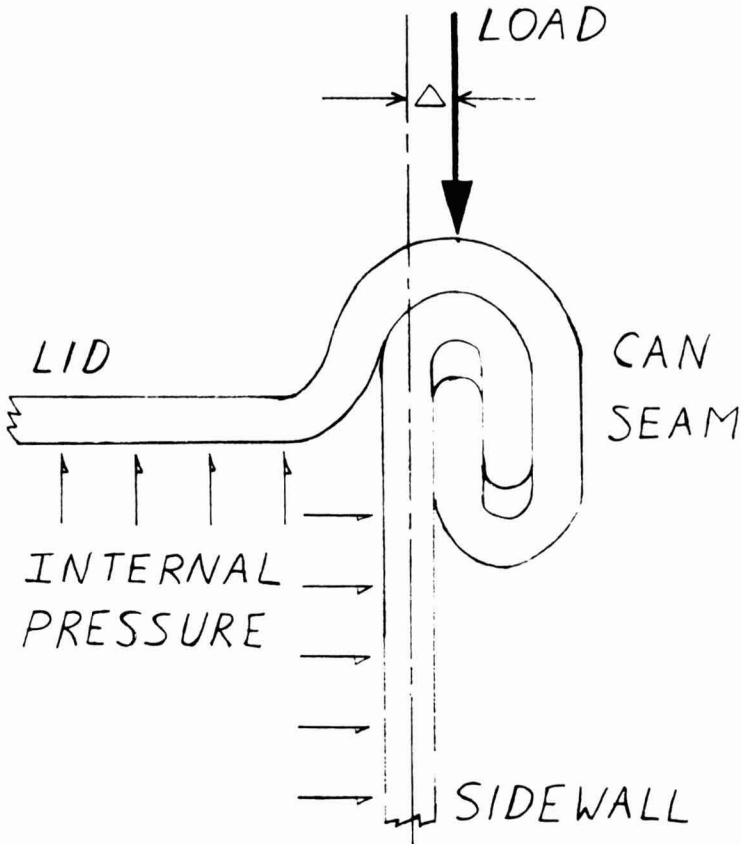


FIG. 4. CAN LOADING

Although the previous discussion applies to steel cans, the aluminum cans also had eccentric loading, although in this case the load occurred inside the radius of the sidewall.

The moment creates an additional stress that is largest right at the edge of the sidewall.

The value of Δ was fitted to the experimental results. When Δ was assumed to be constant it was found to be equal to 1.2 mil. The load resistance values were improved slightly by using a thickness parameter in the expression for Δ , Fig. 5.

The moment due to eccentric loading dramatically reduces the load resistance of the cans. Using the empirical Δ excellent agreement between predicted and experimental results can be obtained, for all of the cans tested.

More involved models of the stresses within compressed cans were also studied (Brewbaker 1986). The sidewall and ends were considered separately under the primary loads of compression and pressure, and then the edge loads and moments

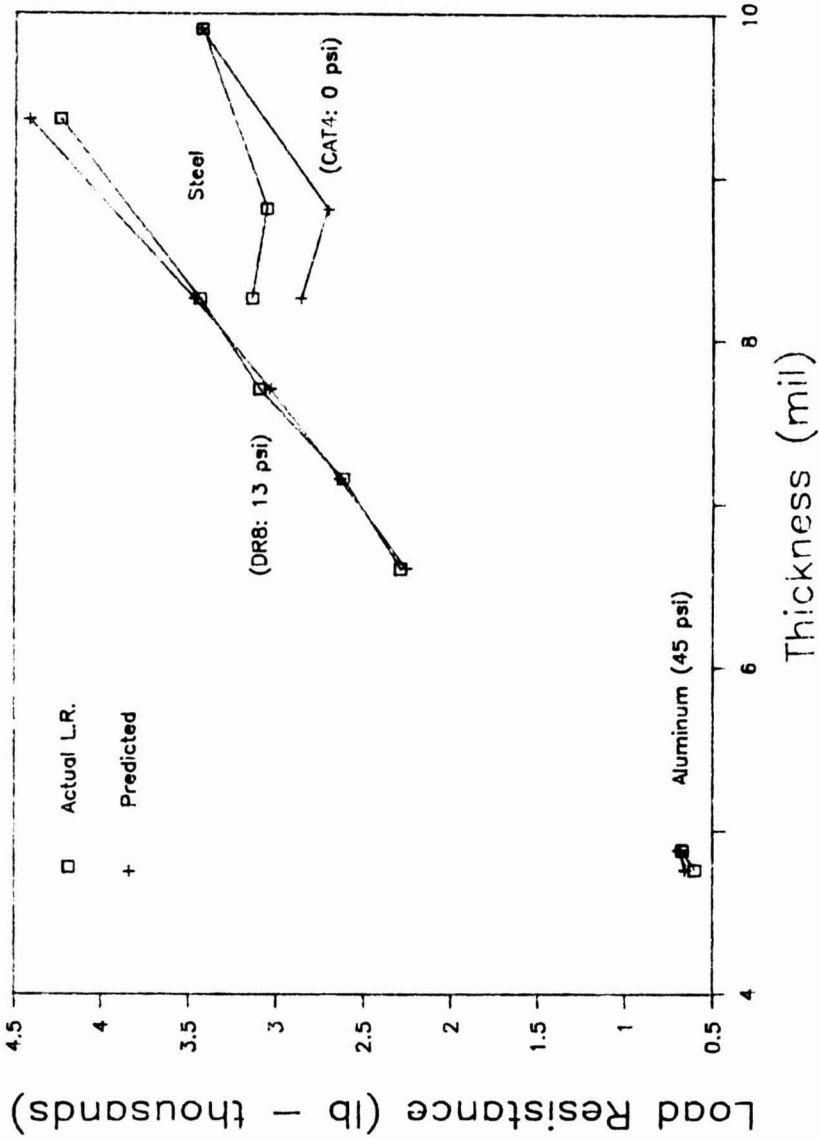


FIG. 5. PREDICTED LOAD RESISTANCES USING ECCENTRIC LOAD CORRECTION
 — for yielding failure

due to their interaction at the junction are calculated, based on the fact that, under these loading conditions, the edge must remain intact. This approach does not match the accuracy of the previous method without including a moment due to eccentric loading. One thing it does predict, however, is an edge moment due to bulging of the can lids under pressure. This would tend to decrease the load resistance of the can as the pressure was increased.

Yielding in Coke-type aluminum cans occurred at the junction between the cylindrical sidewall, and the conical section leading to the upper end. A model was developed which predicts the stresses on the sidewall at this junction due to the primary loads, and the secondary edge loads. Again, it does not predict the actual results without the addition of an eccentric loading effect (Brewbaker 1986). In this case, the eccentricity may be due to the difference at the junction between the model and the actual cans. The model assumes a match between the two sections, the actual cans have a slightly discontinuity.

Figure 6 shows the predicted load resistance of a 4.88 mil 7up aluminum can versus pressure using both the failure mode models. At low pressures, failure would be by buckling, by yielding at higher pressures. Figure 7 shows the situation for a 6.6 mil DR8 steel can, and Fig. 8 for an 8.8 mil CAT4 can. For these cases, the experimental results gave fair agreement.

CONCLUSIONS

The buckling and yielding models just discussed have been designed to be quite general. It is probable that they could be used to predict buckling and yielding in cans of many different sizes and materials, provided they were fairly cylindrical and unbeaded. However, this study only compared the models to one general size of food cans. With this in mind, these models will now be used to predict load and panel resistances in hypothetical food cans of the 303×406 size, the same size as the tests.

Figures 9 and 10 present predicted panel and load resistances versus pressure for three 303×406 Aluminum cans of different thicknesses (4, 6 and 8 mil). Included are the strength standards determined from the study (Brewbaker 1986) for cans currently being used. These standards are 40 psi in panel resistance, and 900 lb in load resistance. As the pressure within the can is increased, less material is required to meet those standards. From Fig. 9, 38 psi of internal pressure is predicted to give a 4 mil Aluminum can an adequate panel resistance. Unfortunately, as seen in Fig. 10, this pressure does not confer the same benefit to the can in load resistance.

Figure 11 summarizes for steel and Aluminum cans of different thicknesses the predicted internal pressures required to meet the strength standards. For DR8 steel cans, panel resistance is the critical parameter. For aluminum cans, panel resistance is important for the thicknesses above 6 mil. Below 6 mil yielding of the can becomes critical.

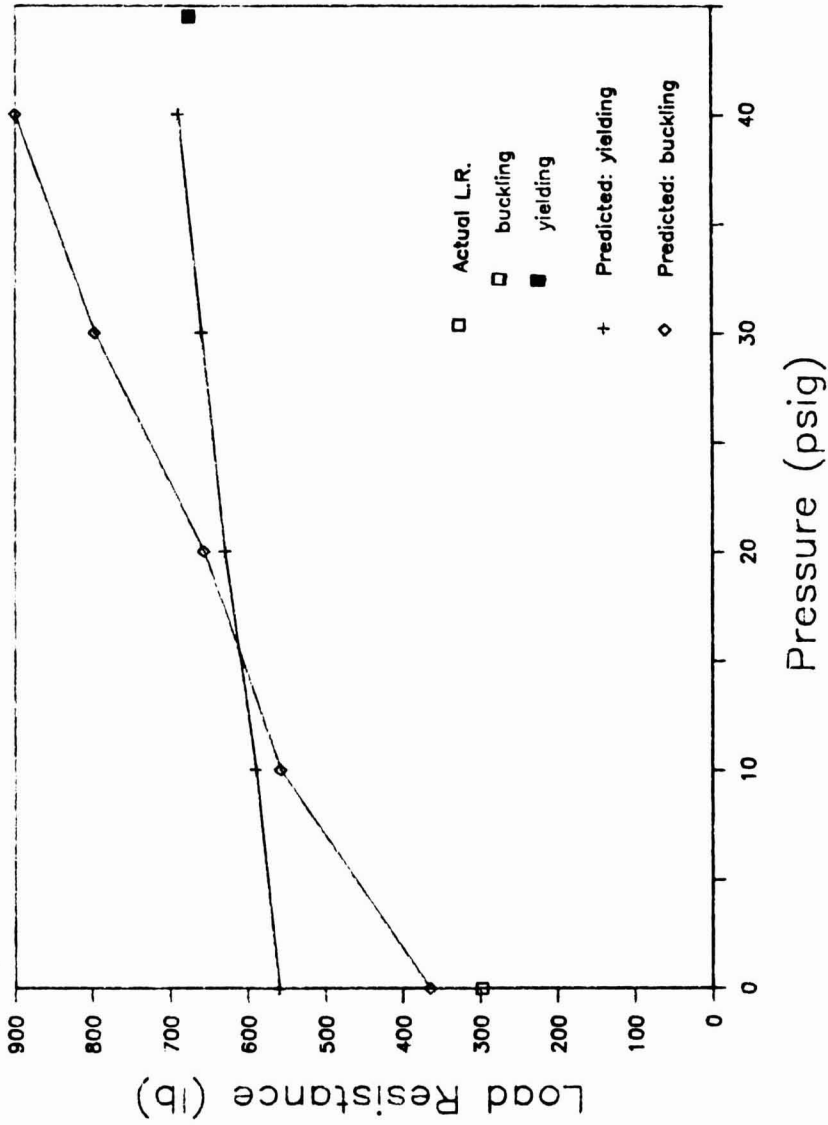


FIG. 6. LOAD RESISTANCE VS PRESSURE — for a 4.88 mil aluminum can

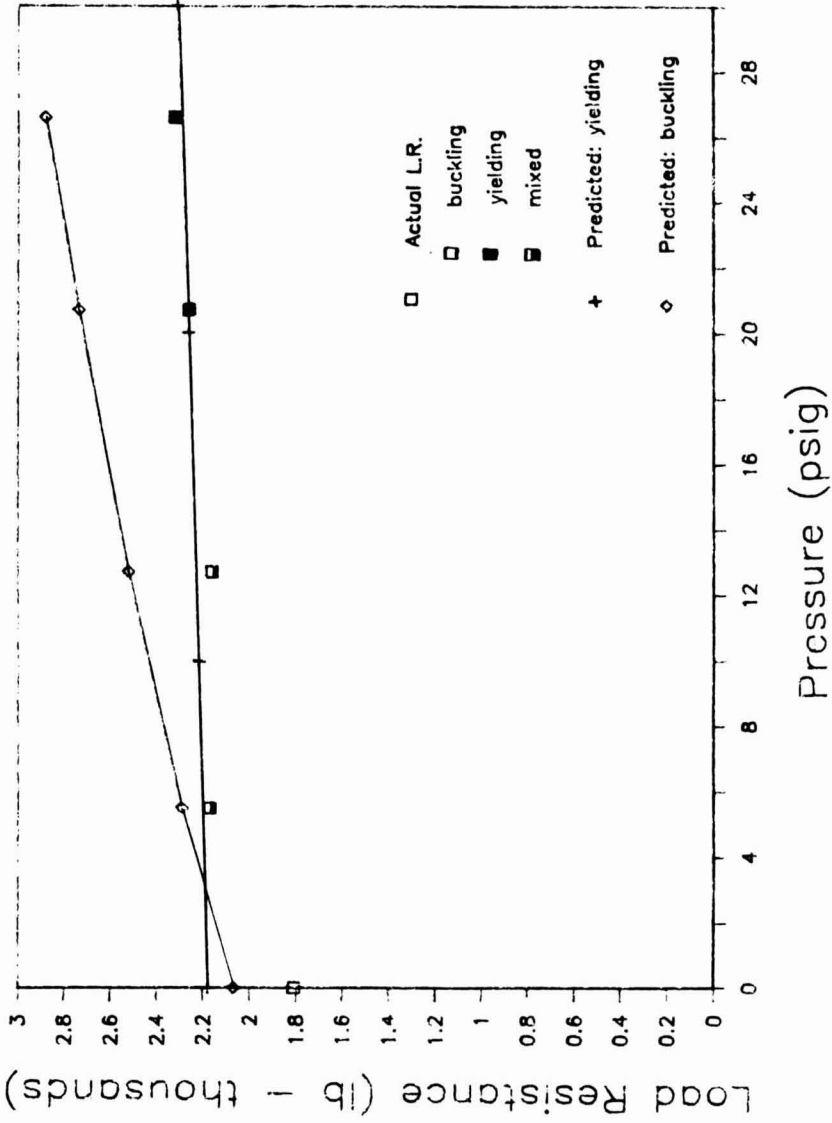


FIG. 7. LOAD RESISTANCE VS PRESSURE — for a 6.6 mil DR8 steel can

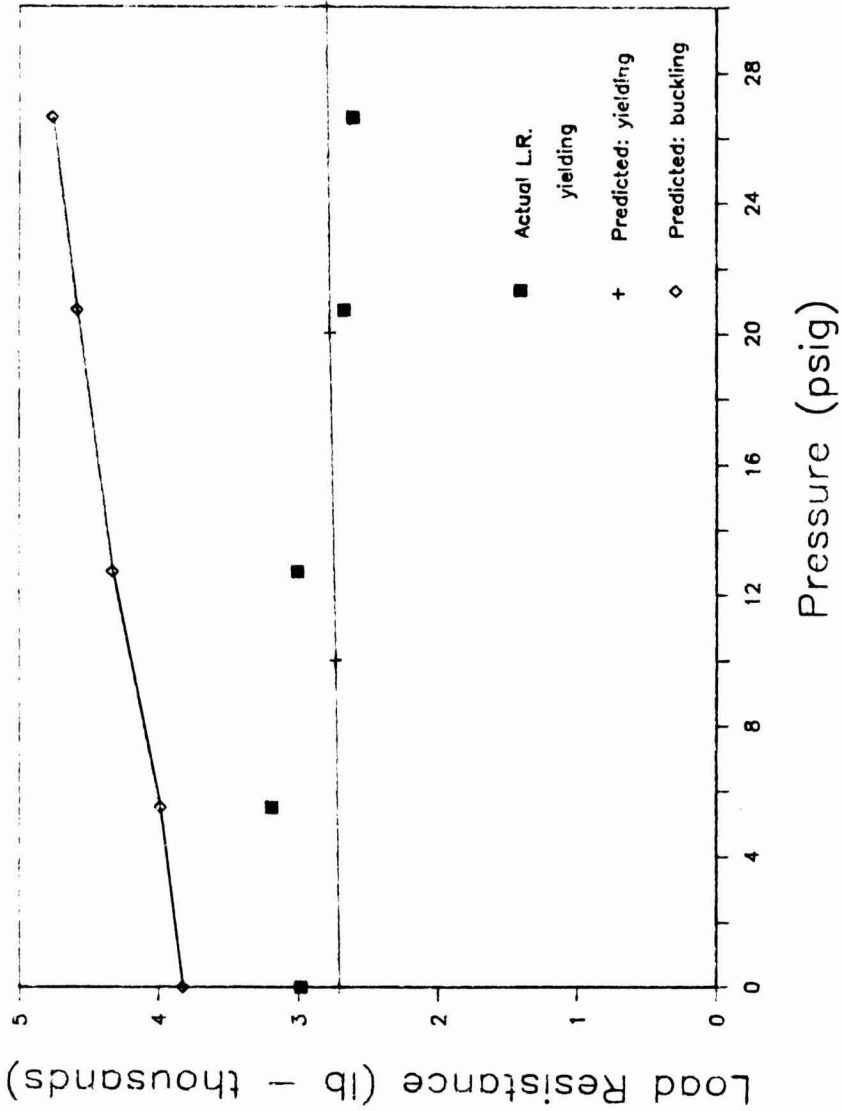


FIG. 8. LOAD RESISTANCE VS PRESSURE — for an 8.8 mil CAT4 steel can

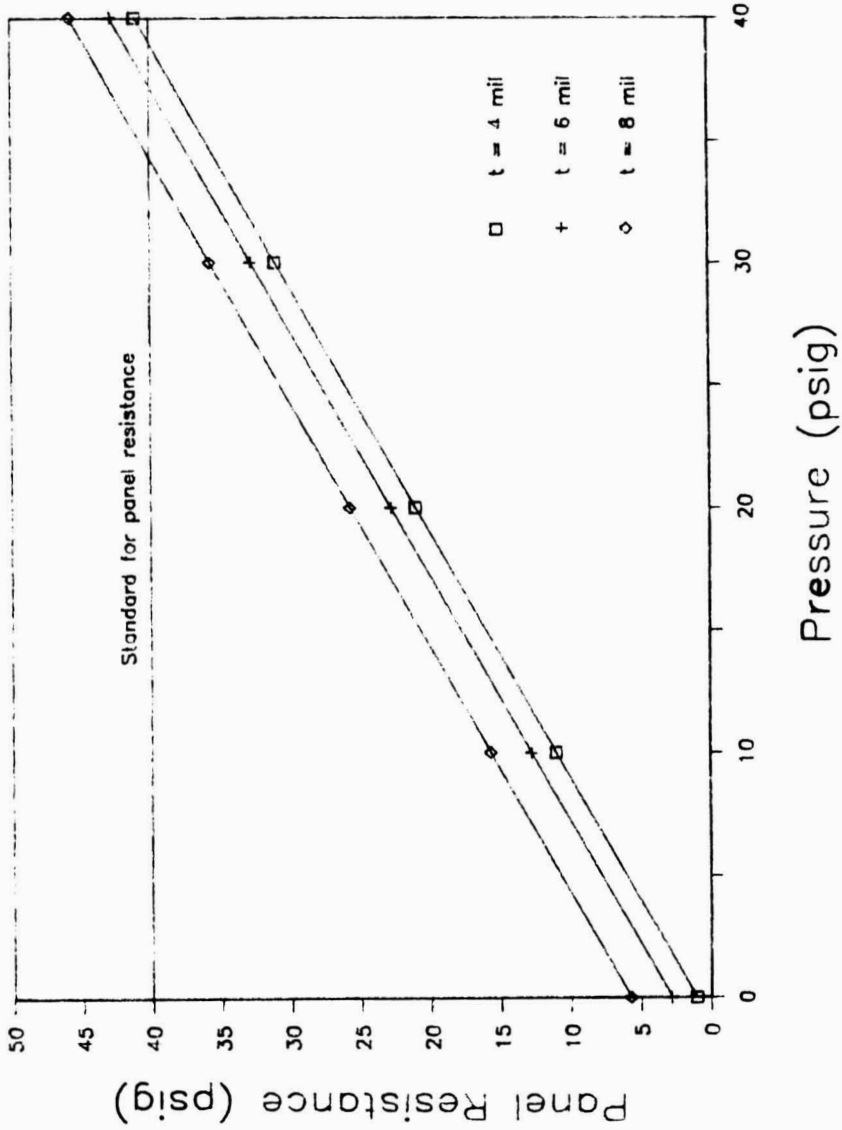


FIG. 9. PANEL RESISTANCE VS PRESSURE — for a 303 x 406 aluminum can

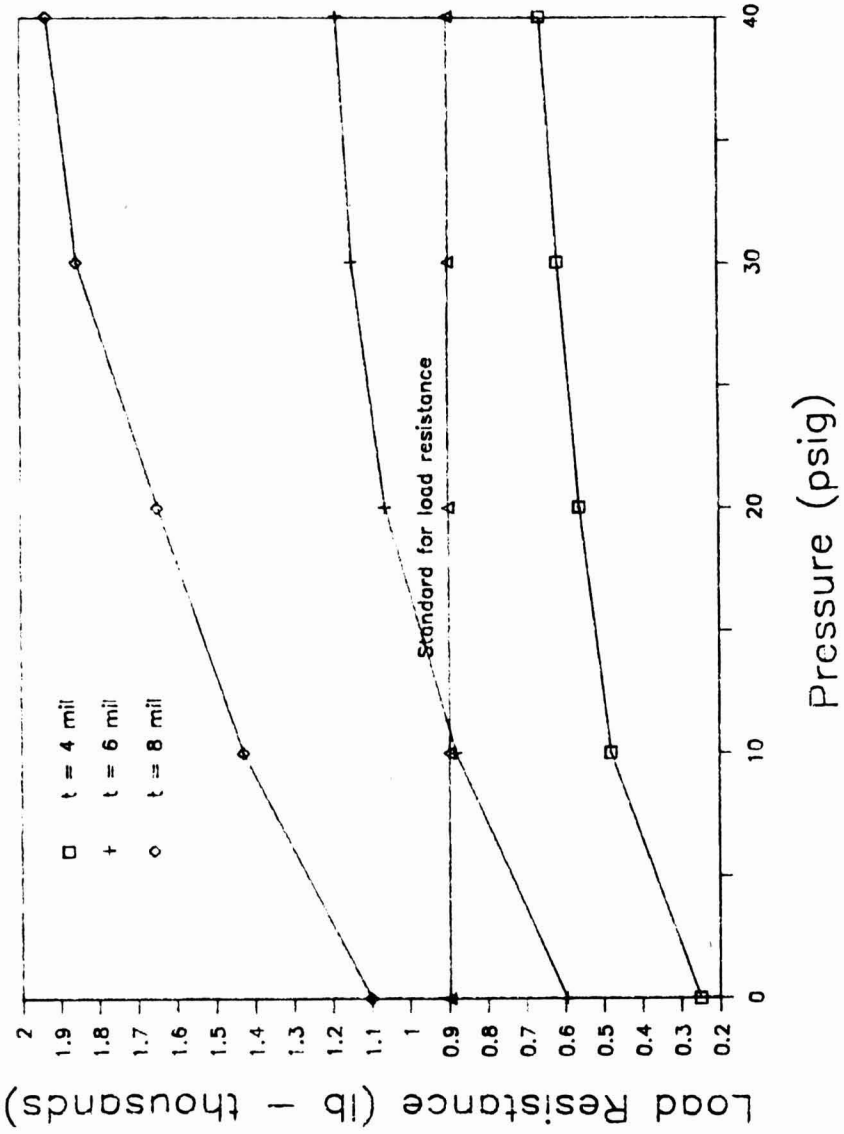


FIG. 10. LOAD RESISTANCE VS PRESSURE — for a 303 x 406 aluminum can

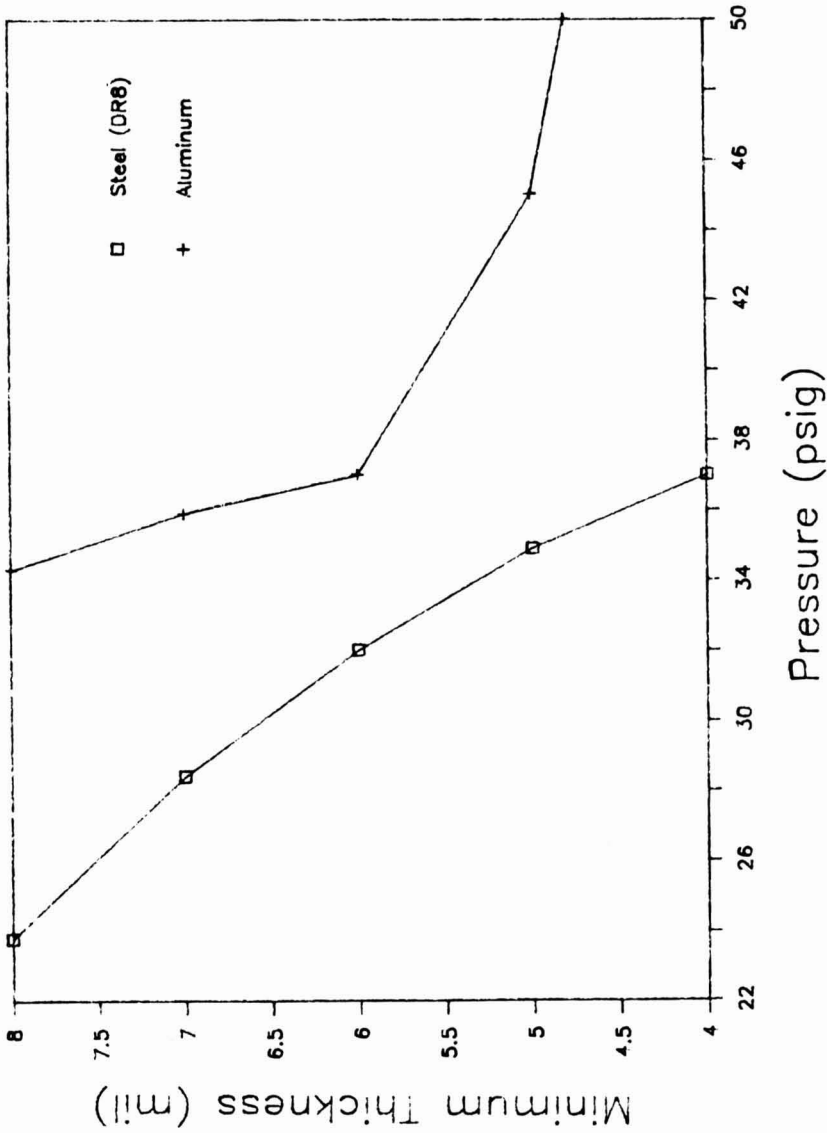


FIG. 11. MINIMUM THICKNESS VS PRESSURE — for unbeaded 303 × 406 cans

Note that for steel cans, increasing the internal pressure to 37 psi allows a decrease in can thickness to 4 mil. For thicknesses below 4 mil other strength considerations may take precedence, such as ease of puncturing or fatigue resistance. For the aluminum cans, the minimum possible thickness may be about 4.8 mil, which would require about 50 psi of internal pressure. Yielding is the critical factor at this point, and lowering the load resistance standard to 800 lb would allow a 4 mil can to be used. For all practical internal pressures, a 4 mil aluminum can would not reach a compression of 900 lb, the standard, without yielding.

Figure 11 is a graphical guide to studying the benefits of pressurized food cans. It can be used to calculate the cost savings of switching to pressurized cans, provided economic data on canning and processing costs were available. For example, the steel in the sidewall of an 8.3 mil can costs about 3.4 cents. For a 6 mil can, this cost is about 2.6 cents (Leonard 1980). According to Fig. 11 then, a material cost savings of over 25% could be gained by pressurizing the can. Of course, this ignores the other costs associated with pressurization.

It is also useful to speculate on material changes. For example, below 6 mil, the cost difference between steel and aluminum cans becomes fairly narrow, and a switch from steel to aluminum could be contemplated (Leonard 1980). Similar graphs could be used to gauge the prospects of plastic cans.

REFERENCES

- BAKER, E.H., KOVALEVSKY, L. and RISH, F.L. 1972. *Structural Analysis of Shells*. McGraw-Hill, New York.
- BREWBAKER, P.L. 1986. Strength Characteristics of Pressurized Cans, Unpublished M.S. Thesis, University of California, Davis.
- HARRIS, L.A., SUER, H.S., SKENE, W.T. and BENJAMIN, R.J. 1957. The stability of thin-walled unstiffened circular cylinders under axial compression including the effects of internal pressure. *J. Aeronautical Sciences*. 24, 587.
- LEONARD, E.A. 1980. *Packaging Economics*. Books for Industry.
- YAMAKI, N. 1984. *Elastic Stability of Circular Cylindrical Shells*. Elsevier Science Publishing Co., Amsterdam.

PUBLICATIONS IN FOOD SCIENCE AND NUTRITION

Journals

JOURNAL OF SENSORY STUDIES, M.C. Gacula, Jr.
 JOURNAL OF FOOD SERVICE SYSTEMS, O.P. Snyder, Jr.
 JOURNAL OF FOOD BIOCHEMISTRY, J.R. Whitaker, N.F. Haard and
 H. Swaisgood
 JOURNAL OF FOOD PROCESS ENGINEERING, D.R. Heldman and R.P. Singh
 JOURNAL OF FOOD PROCESSING AND PRESERVATION, D.B. Lund
 JOURNAL OF FOOD QUALITY, R.L. Shewfelt
 JOURNAL OF FOOD SAFETY, J.D. Rosen and T.J. Montville
 JOURNAL OF TEXTURE STUDIES, M.C. Bourne and P. Sherman
 JOURNAL OF NUTRITION, GROWTH AND CANCER, G.P. Tryfiates

Books

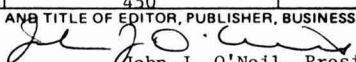
QUALITY ASSURANCE OF FOODS, J.E. Stauffer
 THE SCIENCE OF MEAT AND MEAT PRODUCTS, 3RD ED., J.F. Price and
 B.S. Schweigert
 HANDBOOK OF FOOD COLORANT PATENTS, F.J. Francis
 ROLE OF CHEMISTRY IN THE QUALITY OF PROCESSED FOODS,
 O.R. Fennema, W.H. Chang and C.Y. Lii
 NEW DIRECTIONS FOR PRODUCT TESTING AND SENSORY ANALYSIS
 OF FOODS, H.R. Moskowitz
 PRODUCT TESTING AND SENSORY EVALUATION OF FOODS,
 H.R. Moskowitz
 ENVIRONMENTAL ASPECTS OF CANCER: ROLE OF MACRO AND MICRO
 COMPONENTS OF FOODS, E.L. Wynder *et al.*
 FOOD PRODUCT DEVELOPMENT IN IMPLEMENTING DIETARY
 GUIDELINES, G.E. Livingston, R.J. Moshy, and C.M. Chang
 SHELF-LIFE DATING OF FOODS, T.P. Labuza
 RECENT ADVANCES IN OBESITY RESEARCH, VOL. V, E. Berry,
 S.H. Blondheim, H.E. Eliahou and E. Shafrir
 RECENT ADVANCES IN OBESITY RESEARCH, VOL. IV, J. Hirsch *et al.*
 RECENT ADVANCES IN OBESITY RESEARCH, VOL. III, P. Bjorntorp *et al.*
 RECENT ADVANCES IN OBESITY RESEARCH, VOL. II, G.A. Bray
 RECENT ADVANCES IN OBESITY RESEARCH, VOL. I, A.N. Howard
 ANTINUTRIENTS AND NATURAL TOXICANTS IN FOOD, R.L. Ory
 UTILIZATION OF PROTEIN RESOURCES, D.W. Stanley *et al.*
 FOOD INDUSTRY ENERGY ALTERNATIVES, R.P. Ouellette *et al.*
 VITAMIN B₆: METABOLISM AND ROLE IN GROWTH, G.P. Tryfiates
 HUMAN NUTRITION, 3RD ED., F.R. Mottram
 FOOD POISONING AND FOOD HYGIENE, 4TH ED., B.C. Hobbs *et al.*
 POSTHARVEST BIOLOGY AND BIOTECHNOLOGY, H.O. Hultin and M. Milner

Newsletters

FOOD INDUSTRY REPORT, G.C. Melson
 FOOD, NUTRITION AND HEALTH, P.A. Lachance and M.C. Fisher
 FOOD PACKAGING AND LABELING, S. Sacharow

STATEMENT OF OWNERSHIP, MANAGEMENT AND CIRCULATION

Required by 39 U.S.C. 3685)

1A. TITLE OF PUBLICATION Journal of Food Process Engineering		1B. PUBLICATION NO. 0 1 4 5 8 8 7 6						2. DATE OF FILING Oct. 1, 1987
3. FREQUENCY OF ISSUE Quarterly		3A. NO. OF ISSUES PUBLISHED ANNUALLY 4				3B. ANNUAL SUBSCRIPTION PRICE \$80.00		
4. COMPLETE MAILING ADDRESS OF KNOWN OFFICE OF PUBLICATION (Street, City, County, State and ZIP+4 Code) (Not printers) FOOD & NUTRITION PRESS, INC. 6527 MAIN STREET, POB 583, TRUMBULL, FAIRFIELD, CONNECTICUT 06611								
5. COMPLETE MAILING ADDRESS OF THE HEADQUARTERS OF GENERAL BUSINESS OFFICES OF THE PUBLISHER (Not printer) FOOD & NUTRITION PRESS, INC., 6527 MAIN STREET, POB 583, TRUMBULL, CONNECTICUT 06611								
6. FULL NAMES AND COMPLETE MAILING ADDRESS OF PUBLISHER, EDITOR, AND MANAGING EDITOR (This item MUST NOT be blank)								
PUBLISHER (Name and Complete Mailing Address) John J. O'Neil, 6527 Main Street, POB 583, Trumbull, Connecticut 06611								
EDITOR (Name and Complete Mailing Address) Dr. Dennis R. Heldman, National Food Processors Association, 1401 New York Ave., NW Washington, D.C. 20005								
MANAGING EDITOR (Name and Complete Mailing Address) Dr. R. Paul Singh, University of Calif., Dept. of Agricultural Engineering, Davis, CA 95616								
7. OWNER (If owned by a corporation, its name and address must be stated and also immediately thereunder the names and addresses of stockholders owning or holding 1 percent or more of total amount of stock. If not owned by a corporation, the names and addresses of the individual owners must be given. If owned by a partnership or other unincorporated firm, its name and address, as well as that of each individual must be given. If the publication is published by a nonprofit organization, its name and address must be stated.) (Item must be completed.)								
FULL NAME			COMPLETE MAILING ADDRESS					
Food & Nutrition Press, Inc.			6527 Main Street, POB 583, Trumbull, CT 06611					
John J. O'Neil			53 Stonehouse Rd., Trumbull, CT 06611					
Michael J. Tully			3 North Slope, Union Gap Village, Clinton, NJ					
Kathryn O & Christopher R. Ziko			8 Maria Alicia Dr., Huntington, CT 06484					
John J. O'Neil, Jr.			115 Maureen St., Stratford, CT 06497					
8. KNOWN BONDHOLDERS, MORTGAGEES, AND OTHER SECURITY HOLDERS OWNING OR HOLDING 1 PERCENT OR MORE OF TOTAL AMOUNT OF BONDS, MORTGAGES OR OTHER SECURITIES (If there are none, so state)								
FULL NAME			COMPLETE MAILING ADDRESS					
None								
9. FOR COMPLETION BY NONPROFIT ORGANIZATIONS AUTHORIZED TO MAIL AT SPECIAL RATES (Section 423.12 DMM only) The purpose, function, and nonprofit status of this organization and the exempt status for Federal income tax purposes (Check one)								
<input type="checkbox"/> (1) HAS NOT CHANGED DURING PRECEDING 12 MONTHS			<input type="checkbox"/> (2) HAS CHANGED DURING PRECEDING 12 MONTHS			(If changed, publisher must submit explanation of change with this statement.)		
10. EXTENT AND NATURE OF CIRCULATION (See instructions on reverse side)		AVERAGE NO. COPIES EACH ISSUE DURING PRECEDING 12 MONTHS			ACTUAL NO. COPIES OF SINGLE ISSUE PUBLISHED NEAREST TO FILING DATE			
A. TOTAL NO. COPIES (Net Press Run)		450			450			
B. PAID AND/OR REQUESTED CIRCULATION								
1. Sales through dealers and carriers, street vendors and counter sales		0			0			
2. Mail Subscription (Paid and/or requested)		310			303			
C. TOTAL PAID AND/OR REQUESTED CIRCULATION (Sum of 10B1 and 10B2)		310			303			
D. FREE DISTRIBUTION BY MAIL, CARRIER OR OTHER MEANS SAMPLES, COMPLIMENTARY, AND OTHER FREE COPIES		44			39			
E. TOTAL DISTRIBUTION (Sum of C and D)		354			342			
F. COPIES NOT DISTRIBUTED								
1. Office use, left over, unaccounted, spoiled after printing		96			108			
2. Return from News Agents		0			0			
G. TOTAL (Sum of E, F1 and 2—should equal net press run shown in A)		450			450			
11. I certify that the statements made by me above are correct and complete		SIGNATURE AND TITLE OF EDITOR, PUBLISHER, BUSINESS MANAGER, OR OWNER  John J. O'Neil, President						

GUIDE FOR AUTHORS

Typewritten manuscripts in triplicate should be submitted to the editorial office. The typing should be double-spaced throughout with one-inch margins on all sides.

Page one should contain: the title, which should be concise and informative; the complete name(s) of the author(s); affiliation of the author(s); a running title of 40 characters or less; and the name and mail address to whom correspondence should be sent.

Page two should contain an abstract of not more than 150 words. This abstract should be intelligible by itself.

The main text should begin on page three and will ordinarily have the following arrangement:

Introduction: This should be brief and state the reason for the work in relation to the field. It should indicate what new contribution is made by the work described.

Materials and Methods: Enough information should be provided to allow other investigators to repeat the work. Avoid repeating the details of procedures which have already been published elsewhere.

Results: The results should be presented as concisely as possible. Do not use tables *and* figures for presentation of the same data.

Discussion: The discussion section should be used for the interpretation of results. The results should not be repeated.

In some cases it might be desirable to combine results and discussion sections.

References: References should be given in the text by the surname of the authors and the year. *Et al.* should be used in the text when there are more than two authors. All authors should be given in the Reference section. In the Reference section the references should be listed alphabetically. See below for style to be used.

DEWALD, B., DULANEY, J.T., and TOUSTER, O. 1974. Solubilization and polyacrylamide gel electrophoresis of membrane enzymes with detergents. In *Methods in Enzymology*, Vol. xxxii, (S. Fleischer and L. Packer, eds.) pp. 82-91, Academic Press, New York.

HASSON, E.P. and LATIES, G.G. 1976. Separation and characterization of potato lipid acylhydrolases. *Plant Physiol.* 57,142-147.

ZABORSKY, O. 1973. *Immobilized Enzymes*, pp. 28-46, CRC Press, Cleveland, Ohio.

Journal abbreviations should follow those used in *Chemical Abstracts*. Responsibility for the accuracy of citations rests entirely with the author(s). References to papers in press should indicate the name of the journal and should only be used for papers that have been accepted for publication. Submitted papers should be referred to by such terms as "unpublished observations" or "private communication." However, these last should be used only when absolutely necessary.

Tables should be numbered consecutively with Arabic numerals. The title of the table should appear as below:

Table 1. Activity of potato acyl-hydrolases on neutral lipids, galactolipids, and phospholipids
Description of experimental work or explanation of symbols should go below the table proper. Type tables neatly and correctly as tables are considered art and are not typeset. Single-space tables.

Figures should be listed in order in the text using Arabic numbers. Figure legends should be typed on a separate page. Figures and tables should be intelligible without reference to the text. Authors should indicate where the tables and figures should be placed in the text. Photographs must be supplied as glossy black and white prints. Line diagrams should be drawn with black waterproof ink on white paper or board. The lettering should be of such a size that it is easily legible after reduction. Each diagram and photograph should be clearly labeled on the reverse side with the name(s) of author(s), and title of paper. When not obvious, each photograph and diagram should be labeled on the back to show the top of the photograph or diagram.

Acknowledgments: Acknowledgments should be listed on a separate page.

Short notes will be published where the information is deemed sufficiently important to warrant rapid publication. The format for short papers may be similar to that for regular papers but more concisely written. Short notes may be of a less general nature and written principally for specialists in the particular area with which the manuscript is dealing. Manuscripts which do not meet the requirement of importance and necessity for rapid publication will, after notification of the author(s), be treated as regular papers. Regular papers may be very short.

Standard nomenclature as used in the engineering literature should be followed. Avoid laboratory jargon. If abbreviations or trade names are used, define the material or compound the first time that it is mentioned.

EDITORIAL OFFICES: DR. D.R. HELDMAN, COEDITOR, *Journal of Food Process Engineering*, National Food Processors Association, 1401 New York Avenue, N.W., Washington, D.C. 20005 USA; or DR. R.P. SINGH, COEDITOR, *Journal of Food Process Engineering*, University of California, Davis, Department of Agricultural Engineering, Davis, CA 95616 USA.

CONTENTS

Residence Time Distribution in Horizontal Thin Film Scraped Surface Heat Exchanger (SSHE)
H. ABICHANDI and S.C. SARMA71

Freezing Time Calculation for Products with Simple Geometrical Shapes
C. LACROIX and F. CASTAIGNE81

Thermal Conductivity of Concentrated Whole Milk
G.R. MORE and S. PRASAD105

Heat Transfer in Thin-Film Wiped-Surface Evaporation of Model Liquid Foods
K. STANKIEWICZ and M.A. RAO113

Experimental Verification and Use of Pressurized Can Models
P.L. BREWBAKER and J.M. HENDERSON133